THESIS FOR THE DEGREE OF DOCTOR OF PHILOSOPHY (Ph.D.)

Characterization of distinct molecular genetic alterations in *BRAF* and *NRAS* mutated human primary melanoma

by Viktória Lázár

Supervisor: Margit Balázs, PhD, DSc

UNIVERSITY OF DEBRECEN

DOCTORAL SCHOOL OF HEALTH SCIENCES

DEBRECEN, 2013

Contents

Abbreviations

AKT:	v-akt murine thymoma viral oncogene homolog (also known as protein kinase B, PKB)
BAC:	bacterial artifical chromosome
BRAF:	v-raf murine sarcoma viral oncogene homolog B1
BRAFmut:	primary melanoma tumors harboring BRAF mutation
BRAFWT:	primary melanoma tumors without BRAF mutation which also includes tumors with NRAS mutation
BRN2:	POU class 3 homeobox 2
CAMK:	Ca2+/ calmodulin-dependent protein kinase
CCND1:	Cyclin D1
Cdc42:	cell division control protein 42
CGH:	comparative genomic hybridization
COS2:	Costal 2
DCT:	dopachrome tautomerase (dopachrome delta-isomerase, tyrosine-related protein 2)
EGF/MAPK:	Mitogen-activated protein kinase pathway
ERK1-2:	mitogen activated protein kinase 1-2
FU:	serine/threonine kinase 36
FZ:	Frizzled is a family of G protein-coupled receptor
GF:	growth factor
GLI1:	GLI family zinc finger 1
G protein	Guanine nucleotide-binding proteins
GRB2:	growth factor receptor-bound protein 2
GTP	Guanosine-5'-triphosphate
HH:	Hedgehog pathway
HRAS:	v-Ha-ras Harvey rat sarcoma viral oncogene homolog
IGF:	Insulin-like Growth Factor pathway
JAK:	Janus Activating Kinase pathway
JNK:	c-Jun N-terminal kinases
LRP:	the LDL receptor–related protein
MEK1-2:	mitogen-activated protein kinase kinase 1-2
MITF:	microphthalmia-associated transcription factor

MYC:	v-myc myelocytomatosis viral oncogene homolog
NHR:	Nuclear Hormone Receptor
NOTCH:	Notch pathway
NRAS:	neuroblastoma RAS viral (v-ras) oncogene homolog
NRASmut:	primary melanoma tumors harbouring NRAS mutation
PDK1:	phosphoinositide-dependant kinase 1
PI3K:	phosphatidylinositol 3-kinase
PIP2:	phosphatidylinositol (4,5)-bisphosphate
PIP3:	phosphatidylinositol (3,4,5)-trisphosphate
PKC:	protein kinase C
PTCH1:	transmembrane receptor Patched1
RAF:	v-raf murine sarcoma 3611 viral oncogene homolog (ARAF), v-raf murine sarcoma viral oncogene homolog B1 (BRAF), v-raf-1 murine leukemia viral oncogene homolog 1 (RAF1)
RAS:	v-Ha-ras Harvey rat sarcoma viral oncogene homolog (HRAS), v-Ki-ras2 Kirsten rat sarcoma viral oncogene homolog (KRAS), neuroblastoma RAS viral (v-ras) oncogene homolog (NRAS)
SMO:	smoothened, frizzled family receptor
SSM:	superficially spreading melanoma
NM:	nodular melanoma
SUFU:	Suppressor of Fu
UV:	ultraviolet
WNT:	Wingless pathway
WT:	primary melanoma tumors without BRAF or NRAS mutations

Introduction

Malignant melanoma is the third most frequent type of skin cancer and it is one of the most malignant tumors, accounting for only about 5% of skin cancer cases but 65% of skin cancer deaths [1]. Melanoma originates from melanocytes which derived from neural crest progenitors that migrate to the basal layer of the epidermis during embryonic development [2]. Each melanocyte develops an intimate relationship with many keratinocytes [3]. Keratinocytes regulate melanocytes survival, differentiation and proliferation via secretion of different factors and melanocytes transfer packets of melanin pigment (melanosomes) to them [4]. Melanosomes form a cap-like structure in order to absorb ultraviolet radiation and prevents the direct mutagenic effects of ultraviolet radiation generated free radicals [5].

The major cause of death from melanoma is distant metastasis. Melanoma has a remarkable ability to spread via the blood stream to almost any area of the body, the most common organs are the lungs, brain, bones and liver. As soon as the first distant metastasis appears, the disease becomes one of the most aggressive and chemoresistant tumors [6]. The common clinical therapies in the treatment of metastatic melanoma, that are approved by the Food and Drug Administration such as dacarbazine (DTC) and interleukin 2 have not been shown to improve the median overall survival [7].

Melanoma develops as a result of accumulated molecular alterations in several important genetic pathways in melanocyte and as a result of loss of the tight-knit regulation from keratinocytes leading to a continuous production of melanin [8]. These abnormalities promote uncontrolled cell proliferation and escape of melanoma cells from programmed cell death in response to DNA damage. It is thought that tumor cell evolution is an enormously diverse, unpredictable, stochastic process, on the other hand, it is also known that during tumor genesis, different chromosomal abnormalities occur either singly or in combination, in a distinctly nonrandom pattern. There is a hypothesis that epigenetic and genetic alterations in tumors are clonally selected in a fashion that is not independent. Cells in neoplasms compete for resources, such as oxygen and glucose, as well as space. Thus, tumor cells that acquired mutations that increased their fitness will spread in the neoplasm. In this way, a population of mutant cells, called a clone, can expand in the neoplasm. [9]

Activation of the mitogen-activated protein kinase (MAPK) pathway through mutations in BRAF or NRAS is a common event in primary cutaneous melanoma. However, until now there is only few studies focusing on BRAF or NRAS mutated primary melanoma subtypes in which genome wide investigations were performed [10, 11]. BRAF and NRAS mutation arise

early during melanoma pathogenesis and it is proven that they are preserved throughout tumor progression and contribute to invasive melanoma but only in conjunction with other mutations.

Therefore the main objective of this work was to evaluate those non-random genetic alterations which can properly differentiate between these important subtypes of melanomas (i.e. a) primary melanomas with a) BRAF or b) NRAS mutations and c) wild type for both loci. For this purpose high-resolution array comparative genomic hybridization was used to evaluate copy number changes in a series of primary cutaneous melanomas. Array CGH (array comparative genomic hybridization) identifies genomic imbalance at a level of resolution higher than that achievable by classical cytogenetic analysis. The higher resolution of genomic screening has allowed a more detailed evaluation of DNA copy number alterations.

Amplification of the 11q13 chromosomal region is a common event in primary melanomas. Several candidate genes are localized at this sequence; however, their role in melanoma has not been clearly defined yet. Another aim of this study was to develop an accurate method for determining the amplification pattern of six candidate genes that map to the 11q13 amplicon core and to elucidate the possible relationship between BRAF, NRAS mutations and CCND1 copy number alterations, all of which are key components of the MAP kinase pathway.

Recent advances in the understanding of the prevalence and patterns of BRAF and NRAS mutation in melanoma have led to impressive results in clinical trials of personalized, targeted therapies for this disease [12]. In spite of the fact that it is curative, some side effects, such as development of SCC (squamous cell carcinoma), as well as tumour resistance and recurrence, are common limitations of this therapeutic strategy. Therefore, it is clear that novel treatments are desperately needed. The investigation of additional oncogenic events which are associated with BRAF mutations can provide rational additional targets for combination therapy and this was not investigated yet. Improved understanding of melanoma biology and better tumor classification strategies based on molecular changes enables a more refined multi-target drug selection in malignant melanoma treatment which can lead to more effective therapeutic approaches. A long term goal would be in the future that with the help of this genetic predisposition reflected in specific patterns of copy number alterations, subgroups of patients could be identified that differ in prognosis or in the response of available therapeutic strategies.

1. Cutaneous malignant melanoma

1.1.Epidemiology

Both the incidence and mortality rates associated with malignant melnoma continue to rise in all Caucasian populations, and despite improved survival, the death rates continues to climb. Thus, it will be a major public health problem in the near future, which motivates efforts to determine genetic and environmental factors driving melanoma genesis and progression [13].

Since the mid-1960s, melanoma incidence has risen by 3-8% per year in most European countries [14]. The most likely explanation for the rise in incidence rates is partly due to increased awareness and earlier diagnosis of thin melanomas and hence in a curable stage and partly to increased exposure to solar UV radiation during the past 50 years. Even though the early recognition of cutaneous melanoma is improved, the mortality rate has not changed, it shows a stabilization in Australia, Europe and USA [15].

The incidence rates for melanoma show substantial variation worldwide. It varies by latitude and altitude, with areas closer to the equator and higher in altitude generally having higher rates (Figure 1). It depends on the pigmentation of the population, and their sun exposure patterns. The incidence of malignant melanoma appears to be more common in white populations then in dark skin individuals (Africans, Native Americans, Asians and Hispanics), possibly related to protection from ultraviolet radiation (UVR) provided by melanin [16].

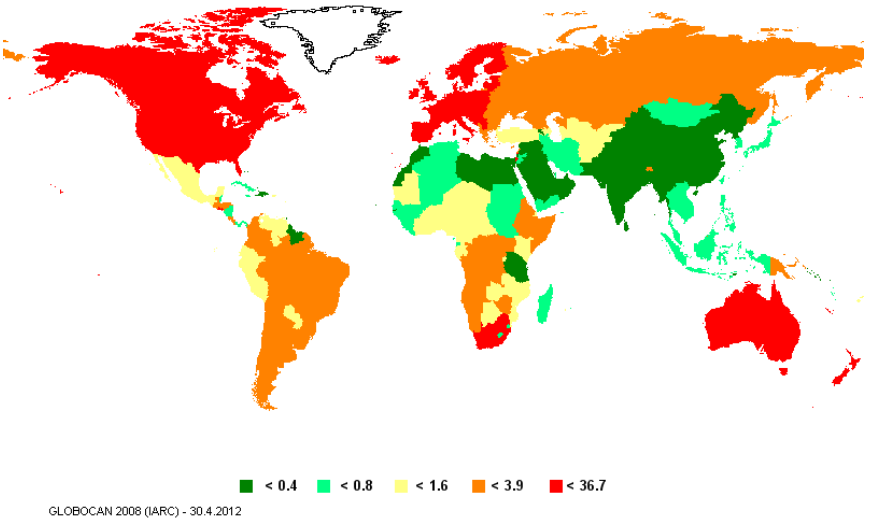

Figure 1. Estimated age-standardised incidence rate per 100 000 of melanoma in both sexes. The figure was downloaded from CANCERMondial (GLOBOCAN DATABASES 2008, Retrieved April 2012 from this website: http://www-dep.iarc.fr/).

In Hungary, 149 and 377 new cases of primary melanoma were documented in 1998 and in 2008, respectively which accounts for 153% increase in ten years [17]. Superficial melanoma was found the most frequent histological type (52 and 54%) followed by nodular melanoma subtype (31% and 23%).

1.2. Melanoma tumor progression

Tumor progression is a multistep process and it generally takes many years for a cancer to develop. We do not know the exact number but it is assumed that probably less than ten genetic changes such as upregulated and inactivated genes required for a normal cell to become a fully malignant cell [18]. Aspects of the malignant phenotype include self-sufficiency of growth signal, insensitivity to growth-inhibitory signals, escape from apoptosis, uncontrolled cell division, stimulation of blood vessel growth, evasion of the immune response, tumor invasion and metastasis.

Metastasis is a clonally selective process. Studies of genetic and epigenetic heterogeneity within tumors support this hypothesis. The clonal selection model of metastasis suggests that cell populations with all of the prerequisites for metastatic capacity are the subpopulations that metastasize [19]. Metastatic cells have the abilities to survive in the circulation and discharge or escape from blood vessel into distant tissues.

Five distinct steps have been proposed for the progression of melanoma, based on clinical and histopathological features (Figure 2) [20]. Step 0, common acquired and congenital nevi with normal melanocytes. Step 1, dysplastic (atypical) nevi: they are generally larger than ordinary moles and have irregular borders. Their colour frequently is not uniform and ranges from pink to dark brown they usually partly raised above the skin surface [21]. Step 2, radial growth phase-(RPG-) confined primary melanoma: confined to the epidermis (melanoma in situ, non invasive). Step 3, radial growth phase (RGP) primary melanoma: melanoma grows out into skin on the side but only slightly down into the skin layers. They are easily cured by surgical removal. Step 4, vertical growth phase (VGP): melanoma is growing vertically or deeper into the tissues and can efficiently adapted to a metastatic phenotype. Step 5, metastatic melanoma: it is an incurable disease with high mortality rate. The reason for it is its high resistance to chemotherapy and radiotherapy. The average survival is less then 1 year [22]. However, as other neoplasm, some of them can skip steps during their development [20].

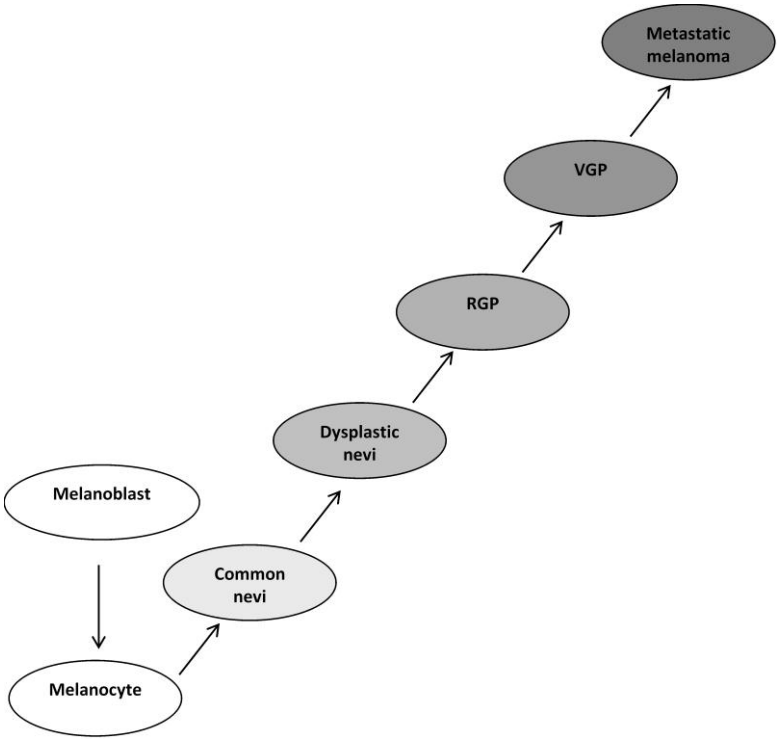

Figure 2. Melanoma tumor progression. The model, developed by Clark, Elder, and Guerry [19], implies that melanoma commonly develops and progresses in a sequence of steps from nevic lesions which can be histologically identified. However, melanoma may also develop directly from normal cells. This figure was modified from Meier et al. (*Front Biosci* 1998, 3:D1005-1010) [20].

Early diagnosis and treatment can prevent death for the majority of these patients. The prognosis in melanoma is directly linked to the depth of this neoplasm; it means that detection of melanoma early is crucial importance in saving lives.

1.3.Histological subtypes

There are four histological subtypes of cutaneous melanoma. Among them the most common are superficially spreading melanoma (SSM) and nodular melanoma (NM), which constitute 88% of tumors, the next 8% consisting of lentigo maligna melanoma (LMM) and acral lentigious melanoma (ALM). SSM represents about 70% of cutaneous melanoma and NM accounts for approximately 10-15% of cases [23]. Superficial spreading melanomas arise *de novo* or in association with a nevus and more often occur on sun-exposed skin, particularly on areas of intermittent sun exposure such as on the back of the leg and on the back [24]. Nodular melanoma has no radial growth phase and therefore progresses in a more aggressive manner; and they often fail to be diagnosed, therefore it can be difficult to recognize in the early stage of their development. Lentigo maligna melanoma is a subtype of melanoma in situ, it occurs on sun-exposed skin such as on face and upper extremities and represents 5-15% of the

cases[25]. Acral lentigious melanoma is a form of lentiginous melanoma which typically develops on the feet, hands, toenails, fingernails, and inside mucous membranes. It is a rare malignancy which accounts for only 5% of melanoma cases and it is often diagnosed at a later stage and has a poorer prognosis than cutaneous melanoma [26]. One of the rare variants of malignant melanoma are the desmoplastic melanomas which represents 1-3% of melanomas and occur in older age group, and are more common on the head and neck and often amelanotic [27].

1.4. Prognostic factors and staging system

One of the most important prognostic factors is the disease stage at the time of diagnosis. The Americtan Joint Committee on Cancer (AJCC) staging system for melanoma was introduced in 2002 and now it has become widely used internationally. It was based on the details of 17 600 melanoma patients from all around the world [28, 29]. This system distinguishes four different disease stages. Clinical stages I and II are confined to patients who has no evidence of metastasis after clinical or radiological examination. Primary melanomas with Breslow thickness less than 1.01 mm with or without ulceration and less than 2.01 mm without ulceration were defined to be at stage I. Ulceration was included as a criterion for staging. Stage II were designated as those with primary tumors, where the tumor thickness were greater than 1.0 mm with ulceration or greater than 2.0 mm with or without ulceration. Stage III is characterized by any tumor thickness with ulceration and 1-3 microscopic positive nodes or any tumor thickness without ulceration and 1-3 macroscopic positive nodes. Stage IV melanoma patients have metastases at a distant site [30].

In Stage I and II localized melanoma tumor thickness according to Breslow, ulceration and Clark level of invasion were the most powerful prognostic factors [31]. Breslow thickness measures tumor thickness in millimeters from the granular cell layer to the deepest part of the tumor in a histological sample [32]. Clark levels (I-IV) refer to how deep the tumor has penetrated into the layers of the skin. So it correlates anatomic level of invasion [33]. Melanomas with a Breslow's depth greater than 1 mm have an increased risk of harboring occult regional metastases.

Other statistically important factors were the following: the patient’s age and gender and the site of primary melanoma. Many studies have addressed that patients with melanomas on the extremities, have a better prognosis than those with lesions on the trunk, head or neck, except for tumors occurring in the plantar or palmar skin, which have an especially poor prognosis [34]. Other studies assumed that melanoma in women tend to be associated with thin, nonulcerated

tumors on extremities [35, 36]. The age of the patient is another independent prognostic factor for melanoma, higher age correlated with poorer survival regardless of tumor thickness or ulceration [37].

1.5. Melanoma risk factors

It is likely that there is a complex interaction of environmental (exogenous) and endogenous factors that can increase the chance of getting the disease [38]. The likelihood of the melanoma development in a person is highly depending on his or her genotypic and phenotypic characteristics, and posterior exposure to environmental risk factors particularly with sun exposure [39].

1.5.1. Environmental factors

1.5.1.1. Sunlight

Sun exposure appears to be the major determinant of risk for cutaneous melanoma. It is due to the depletion of the ozone layer, allowing penetration of UV rays into the atmosphere but possibly also due to behavioral change (such as increased use of sun or tanning beds) [24].

Ultraviolet (UV) light has strong genotoxic effects to produce DNA damage. Apart from that UV can induce oxidative stress-mediated mutations in the cellular genome through an indirect mechanism [40]. The UV radiation which reaches the earth' surface consist of UVA (320-400 nm) and UVB (280-320 nm). The UVB portion shows a strong carcinogenic effect on the skin. It produces specific DNA damage particularly cyclobutane pyrimidine dimers (CPDs) and pyrimidine (6-4) pyrimidone photoproducts that triggers changes in the conformation of DNA and may induce mutations in the epidermal cells, leading to the development of cancer [41]. UVB is also known to induce oxidative stress through the production of reactive oxygen species (ROS) by activating the riboflavin, tryptophan and porphyrin. In addition, UVB is proven to suppress immune reactions, and establishes tolerance to antigens [42].

People with fair skin who are exposed to sunlight are most at risk. This probably explains why populations in the North Europe are the most affected. The reduction in the ozone layer, with the resulting increase to ultraviolet rays, is also thought to increase the risk of melanoma. Sunburns in childhood are epidemiologically shown to associate with higher risk for melanoma [43].

1.5.2. Host factors

1.5.2.1. Melanocytic nevi

The list of risk factors in developing malignant melanoma is long and includes the presence of more than 50 acquired (common) nevi, more than five dysplastic (atypical) nevi, large congenital nevi and nevi larger than 6 mm [38]. In 25% of cases, melanoma occurs in conjunction with a pre-existing nevus [44]. The presence of dysplastic nevi confer increased risk factor for the development of multiple primary melanomas which often clusters in families [45].

1.5.2.2. Susceptibility genes in melanoma

The genetic basis of melanoma is complex and appears to involve multiple genes. It is now widely believed that certain genes are associated with predisposition to the disease. Population studies revealed that family history of melanoma varied by geographic area from 0.6 to 12.5%, with generally higher percentages in areas of higher melanoma incidence [46, 47]. The most common definition of "positive family history of cancer" is two or more first-degree relatives with melanoma. Until now two genes conferring susceptibility to melanoma have been found within high risk families, CDKN2A and CDK4 (located on 12q13) [47-49]. Both of these genes are important in cell division control.

CDKN2A is located on chromosome 9p21 and acts as a tumor suppressor gene. It encodes two alternatively spliced protein variants: 1) p16(INK4a) important in the retinoblastoma pathway, 2) and p14ARF, important in the p53 pathway. The p16(INK4a) protein regulates G1 phase exit by inhibiting CDK4 mediated phosphorylation of the retinoblastoma protein [50]. The p14ARF is induced in response to hyperproliferative stimuli and is believed to induce p53-dependent cell cycle arrest or apoptosis [51]. The Melanoma Genetics Consortium estimated the penetrance of melanoma among mutation carriers in 80 high-risk families with CDKN2A mutations from Europe, the US, and Australia. Overall, the cumulative risk of melanoma at age 50 was 0.30 and at age 80 was 0.67 [52].

The CDK4 gene is an oncogene and all reported CDK4 mutations were found in exon 2, which codes for the p16 binding site. Mutations in CDK4 generate a mutated protein kinase CDK4 which is unable to bind p16(INK4) [53]. The data for penetrance of melanoma for mutations in CDK4 were identified among two CDK4 families, and the penetrance rate was found to be 63% [54].

Variations in other genes have also been reported with increased risk of melanoma, particularly MC1R (16p24) (the melanocortin 1 receptor gene) which has been shown to play

a crucial role in human pigmentation [55]. Some variants of MC1R confer increased UV-sensitivity by switching the eumelanin synthesis to pheomelanin [56]. Studies have found that red hair and presence of sun sensitivity are associated with specific genetic variations in MC1R resulted in the development of both sporadic cutaneous melanomas and an increased risk of melanoma [57]. Certain MC1R gene sequence variants lead to an increase in the penetrance of CDKN2A mutations from 50% to 84%, and lower the mean age of onset by 20 years [58].

Although commonly mutated during melanocyte proliferation the BRAF and NRAS genes, that encode protein kinases, are not associated with inherited melanoma susceptibility [59].

1.6. Molecular cytogenetics of melanoma

Several studies on chromosomal aberrations, from cytogenetics to chromosomal and array CGH analysis, show a remarkable heterogeneity in genomic alterations. The current knowledge about molecular cytogenetic alterations was recently summarized by Blokx et al (Figure 3) [60].

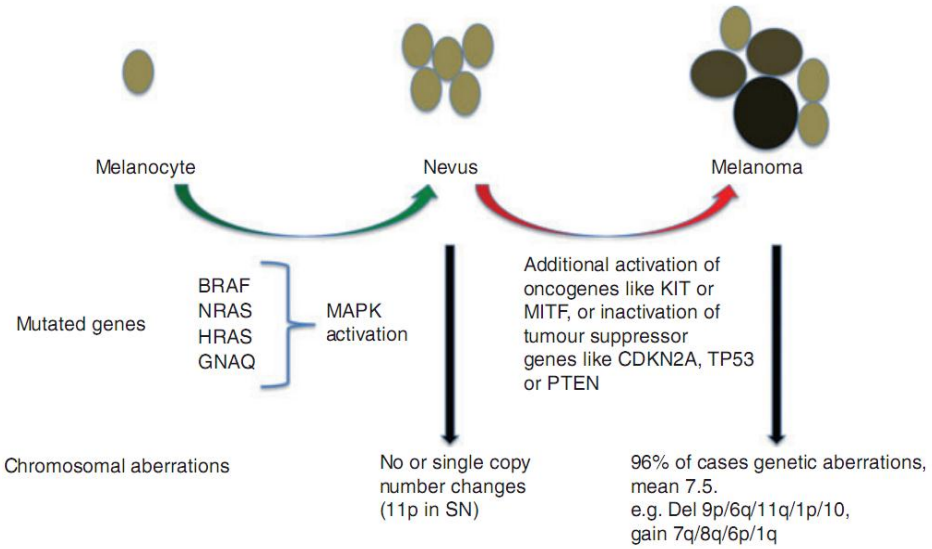

Figure 3. Schematic events in the development of melanocytic tumours from Blokx et al. (*Histopathology* 2010, 56, 121–132) [60]

It is well demonstrated that the development of a normal melanocyte into the malignant phenotype is characterized by certain histological, and so far only incompletely discovered genetic alterations. Activation of the MAPK kinase pathway via somatic mutations in the NRAS and BRAF genes is thought to be one of the first steps in the development of common naevi [61] (see details below in the subsection of "The EGF/MAPK pathway, the role of BRAF

and NRAS mutation" and in Figure 4). Moreover, somatic mutations of the Guanine nucleotide-binding proteins (G protein) (GNAQ) were recently identified in uveal melanomas and blue naevi [62]. These mutations are early events in the development of melanocytic tumours. A number of tumor suppressors and oncogenes were implicated as key factors in the development from melanocytic naevus towards dysplastic naevus, like loss of PTEN, CDKN2A, TP53 and gain of KIT, MITF, CCND1 and MYC [63-67] (Table 1). In sporadic melanoma chromosomal pathogenesis is mainly characterized by widespread aneuploidy [68-70]. Using cytogenetic and loss of heterozygosity studies, several loci was identified as non-random alterations on chromosomes 1p, 6q, 7q, 10q and 11q. Based on CGH data of 132 melanomas the most frequent gains are: 6p, 1q, 7p, 7q, 8q, 17q and 20q; and the most frequent losses were detected on chromosomes 9p, 9q, 10q, 10p, 6q and 11q [71]. (Table 1)

Out of these chromosome alterations three chromosome loci are outstanding in the melanoma prognosis. The first is the 10q23 locus which was found to be more prevalent in the NM subtype and frequently associated with melanoma progression, possibly related to the loss of the tumor-suppressor gene PTEN (10q23.3). This gene is frequently altered in several cancers, such as prostate or colorectal carcinoma [72] (see details below in the subsection of "The PI3K pathway" and in Figure 5).

The second is the chromosome 9p21 which is one of the most frequently altered regions in cutaneous melanoma and as it was mentioned before this is a susceptibility locus for the disease [73]. This genetic locus contains three putative tumor suppressor genes: CDKN2A (with p16 a common alias), CDKN2B (p15 a common alias), and ARF/p14ARF (if distinct from CDKN2A). Using chromosomal comparative genomic hybridization (cCGH), we and others observed that 9p loss was frequently detectable in sporadic primary melanomas, the frequency being between 40% and 80% [11, 71, 74]. It was also observed using array CGH, that 50% of melanomas exhibit CDKN2A deletion and 10% of those cases show homozygous deletion of the gene [11].

The third is the 11q13-q21 chromosome band. There is also a frequent amplification in the majority of primary melanomas[11, 69, 74]. The Cyclin D1 (CCND1) gene has been widely considered to be a target gene in the region because its overexpression is commonly observed in several human cancers, including breast, head and neck, and bladder cancers [75-77]. Beside the CCND1, several other oncogenes and/or cancer-related genes reside within this amplicon core, such as TAOS1, FGF3, FGF4, FGF19 and EMS1 [78-83].

CCND1 is the regulator subunit of cyclin-dependent kinase 4 (CDK4) and cyclin-dependent kinase 6 (CDK6). These enzymes are responsible for phosphorylating the retinoblastoma (Rb) protein and thus promoting cell entry into mitosis. Transcription of CCND1 is stimulated by the MAP kinase pathway, and this is the connection point between the RAS-MAPK- and p16-CCND1/CDK4-Rb pathways [84, 85]. Elevated CCND1 gene copies were found in a large series of acral melanoma subtypes, occasional amplification was described in lentigo maligna melanomas and superficial spreading melanomas (SSM), and only sporadic amplification in the nodular melanoma subtype (NM) [86, 87].

The contribution of the other genes in the 11q13 amplicon to several cancers has been investigated [78-83]. The TAOS1 gene, which is located approximately 12 kb distal to CCND1, was found to be a novel marker for advanced esophageal squamous cell carcinoma and was overexpressed only if its gene amplification was present in the oral squamous cell carcinoma cell lines [79, 83]. Amplification of the EMS1 gene through the overexpression of cortactin protein has been shown to contribute to the invasive potential of tumor cells [81, 88]. This protein is described as an actin-associated scaffolding protein that regulates the formation of actin-based structures closely associated with cell motility [89]. Overexpression of EMS1 causes enhanced cell proliferation, predicts early recurrence and reduced survival in squamous cell carcinoma of the head and neck and in esophageal adenocarcinoma [78, 90, 91]. CCND1 and EMS1 are also thought to be likely to play pathogenic roles in the 11q13 amplicon in bladder tumors [92]. Co-amplification of CCND1, EMS1, FGF3 and FGF4 genes was significantly associated with increased tumor stage and grade in a large series of urinary bladder cancer [82]. However, the possible role of these candidate genes within the 11q13 amplicon has not yet been investigated in primary melanoma.

Table 1. Non-random chromosome alterations related to known onco- or tumor supressor genes

Chromosome region	Onco- or tumorsupressor genes	Event
11q13-q21	CCND1, TAOS1, FGF3, FGF4, FGF19, EMS1	gain
7q34	BRAF	gain
1p13.2	NRAS	gain
12q13.3	CDK4	gain
10q23	PTEN	loss
1q44	AKT3	gain
9p21	CDKN2A	loss
7p13.1	TP53	loss
4q12	KIT	gain
8q24.2	MYC	gain
3p13	MITF	gain

1.7. Genomic profiling of malignant melanoma

The recent development of high-resolution molecular biological techniques such as array CGH have revolutionized our ability to detect genetic alterations in the whole genome which often contain oncogenes whose increased or decreased gene dosage has been selected for during tumor development. Array CGH, it has distinct advantages over classic cytogenetics it allows the rapid detection of copy number changes across the entire genome. It does not require dividing cells and also prior knowledge of specific areas of the chromosome or chromosomes to target via the use of particular probes. The disadvantages of array CGH include the inability to detect balanced chromosomal rearrangements, the detection of copy number variations of uncertain clinical significance, and significantly higher costs than conventional karyotype analysis.

Array comparative genomic hybridization (array CGH) has already been applied on solid tumors; however, using this technique on human primary malignant melanoma is appearing in only few articles. However, there are already some studies showing that genetic data provided by comparative genomic hybridization (CGH) can yield also helpful diagnostic information in melanoma cases which are ambiguous based on histopathologic assessment. One of them compared three Spitz nevi and 2 melanomas and showed the utility of array CGH as a molecular test in distinguishing Spitz nevus from melanoma both of which have overlapping histologic features leading to frequent misdiagnosis[93]. A novel gain at 14q23.2-31.1 was also detected by analyzing the whole genomes of an irinotecan-resistant clones derived from melanoma cells using high resolution array CGH [94]. Another group found concomitant chromosome 7 gain and 10 loss and concomitant 15q22.2-q26.3 gain and 20gain. Moreover, the study revealed discrete copy number alterations associated with mutations in various melanoma genes such as BRAF, NRAS, PTEN and TP53 in 47 different melanoma cell lines using tiling-resolution bacterial artificial chromosome array CGH [95]. After analyzing eleven melanoma metastasis many discreet regions of change - 6q22, 9p21, 6p21, 6p24, 7q31 and 8q24- were uncovered using array CGH [96]. In another study investigators compared autologous melanoma cell lines of clonal derivation with allogeneic ones and correlated array CGH with gene expression profiling to study the dynamics of cancer progression and to identify stable genetic factors for targeted anticancer therapies [97]. Beside that array CGH is highly effective in cataloging recurrent chromosomal numerical aberrations associated with different tumor types in human [98-102] it can also be used to distinguish genetically and histopathologically homogeneous melanomas, predict their ultraviolet (UV)-induced versus

spontaneous etiologies, and identify novel pathogenic lesions such as CDK6 amplification according to a study using mouse models [103].

The largest outcome study of its kind analyzed the genetic alterations and mutational status of BRAF and NRAS in 126 primary melanomas with a relationship to exposure to ultraviolet light. Several marked differences in aberrant genomic regions were found in the groups in which the degree of exposure to the sun differed. The group of melanomas on skin without chronic sun-induced damage frequently had a mutation in BRAF together with chromosome 10 (site of PTEN) loss or mutations in NRAS alone. In contrast, melanomas in the group of tumors arising from skin with chronic sun-induced damage, mucosal melanoma and acral melanoma did not have mutations in BRAF and NRAS but instead had increased numbers of copies of CCND1 or CDK4. These findings indicate distinct genetic pathways in the development of melanoma which will affect the design of targeted therapeutic intervention in the future. Moreover, frequent focused gains involving the CCND1 locus, losses involving chromosome 4q and gains involving regions of chromosome 22 were significantly more common in the group with chronic sun-induced damage than in the group without such damage [11]. In addition, until now only three recent landmark studies investigated the distinct genome-wide alterations in DNA copy number associated with BRAF or NRAS mutation status in primary human melanomas and several melanoma cell lines [10, 95, 104].

1.8.Molecular pathways involved in melanoma progression

This part summarizes the signaling pathways and the most important onco- and tumor suppressor genes involved in melanoma progression. The effect of these genes in melanoma development and therapeutic implications will be also detailed.

1.8.1. The EGF/MAPK pathway, the role of BRAF and NRAS mutation

Molecules of the EGF/MAPK pathway regulate diverse processes ranging from proliferation and differentiation to apoptosis. The EGF/MAPK kinase pathway is initiated through extracellular growth factor stimulation of membrane bound receptor thyrosine kinases (Figure 4). The receptor activates a small G protein called RAS. The Ras proteins belong to the Ras superfamily of small GTPases. There are different mammalian RAS genes such as HRAS (11p15) and NRAS (1p22), etc. In normal cells the Ras proteins transiently activated in response to extracellular growth signals and functions to transduce these signals to intracellular signaling pathways via activation of downstream serine/threonine Raf kinases. NRAS has been shown to activate Raf proteins more efficiently than HRAS [105]. After Raf

protein is activated it phosphorylates and activates mitogen and extracellular signal-regulated protein kinases (MEK1 and MEK2) which activates a third protein kinase called extra cellular signal-regulated protein kinase (ERK) resulting in the activation of transcription factors involved in proliferation, survival and differentiation (Figure 4).

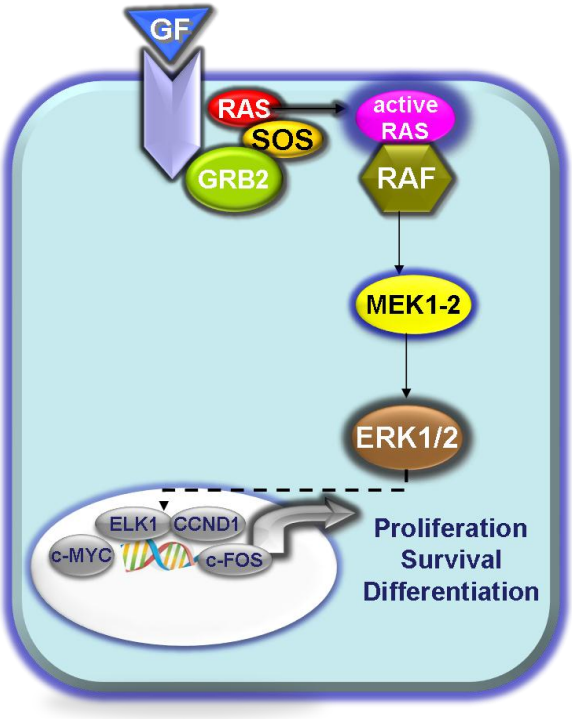

Figure 4: Simplified view of the EGF/MAPK kinase pathway, with emphasis on components implicated in melanoma (Oncogene 2007, 26(22):3279-3290) [76]. Growth factor: **GF**; growth factor receptor-bound protein 2: **GRB2**; v-Ha-ras Harvey rat sarcoma viral oncogene homolog (HRAS), v-Ki-ras2 Kirsten rat sarcoma viral oncogene homolog (KRAS), neuroblastoma RAS viral (v-ras) oncogene homolog (NRAS): **RAS**; v-raf murine sarcoma 3611 viral oncogene homolog (ARAF), v-raf murine sarcoma viral oncogene homolog B1 (BRAF), v-raf-1 murine leukemia viral oncogene homolog 1 (RAF1): **RAF**; son of sevenless: **SOS**, mitogen-activated protein kinase kinase 1-2: **MEK1-2;** mitogen-activated protein kinase 1-2: **ERK1-2**.

There is increasing evidence suggesting a key role for the EGF/MAPK pathway in the development of malignant melanoma. Activation of the mitogen-activated protein kinase pathway through mutations in BRAF or NRAS is a frequent event in the subgroup of cutaneous melanoma [106]. BRAF and NRAS mutation arise early during melanoma pathogenesis and it is proven that they are preserved throughout tumor progression and contribute to invasive melanoma. However it was also found that these mutations are not sufficient to initiate human melanoma *in vivo* [107].

Activating mutations in codon 600 of BRAF (BRAFV600) and in codon 61 of NRAS

(NRASQ61) are, so far, the most common single mutations detected in human cutaneous melanoma [108, 109]. There is also evidence that overexpression of wild-type BRAF is another mechanism underlying constitutive activation of the MAPK pathway that stimulates growth of melanoma cells [110]. The overexpression or constitutive activation of this gene results in activation of ERK and contribute to increased cell proliferation. Previous results from melanoma cohorts interestingly show that mutations in the BRAF and NRAS genes are almost always mutually exclusive suggesting that even though both BRAF and NRAS function as key molecules along the EGF/MAPK pathway; they may cooperate with different oncogenic events during melanoma development [111].

Recent advances in the understanding of the prevalence and patterns of BRAF mutation in melanoma have led to impressive results in clinical trials of personalized, targeted therapies for this disease [112]. A dramatic success was recently demonstrated with the novel small-molecule BRAF inhibitor PLX4032/vemurafenib in metastatic BRAF mutant melanomas. The drug, with patients harboring BRAF V600E mutation induced metastatic melanoma, resulted in complete or partial tumor regression in 81% of patients with an estimated median progression-free survival rate of 7 months [113]. This groundbreaking result provided the first evidence that oncogene-targeted approach is valid for metastatic melanoma.

Cyclin D1 (CCND1) is an important down-stream effector of the MAPK pathway. Protein products of the CCND1 gene play a crucial role in cell cyle regulation [114]. CCND1 is rarely expressed in melanocytic nevi while it is commonly present in primary melanoma [115]. Amplification and/or overexpression of the gene have been found in several types of human tumors including the different subtypes of primary melanomas [11, 116, 117]. Using comparative genomic hybridization (CGH) analysis, we and others found frequent amplification of the 11q13–q21 chromosome band in primary melanomas [11, 69, 74, 118]. High frequency of CCND1 gene amplification was found in a large series of acral melanoma subtypes, occasional amplification in lentigo maligna melanomas and superficial spreading melanomas (SSM), however amplification of CCND1 gene was found only sporadically in nodular melanoma subtype (NM) [86, 87]. Increased CCND1 level was observed to correlate with stage, grade and prognosis in melanoma suggesting an important role of this oncogene in tumor pathogenesis [117]. It was observed that down regulation of CCND1 expression has reduced the melanoma cell growth and induced apoptosis [86]. These results suggested that alterations of the CCND1 gene is an important factor in melanoma progression and might also be an important therapeutic target. However targeting cylcin D1 proteins directly is extremely difficult because the proteins do not have intrinsic enzymatic activity and they are located intranuclear.

Although, there are some possible suggested approaches. One way to do this to target cyclin D1 by inhibiting associated kinases, as CDK4 and CDK6. Second method is a less direct. Several compounds (tamoxifen, transtuzumab, cytotoxics, and radiotherapy) lead to cyclin D1 downregulation or the protein degradation. A third approach can reach a greater specificity by substrate mimetics inhibiting Cyclin D1-CCDK4 protein interaction [119].

1.8.2. The PI3K pathway

Phosphatidylinositol 3-kinases (PI3Ks) evolved from a single enzyme that regulates vesicle trafficking in unicellular eukaryotes into a family of enzymes that has central role in several cellular processes critical for cancer progression, including metabolism, growth, survival, and motility in multicellular organisms [120] (Figure 5). Inappropriate PI3K signalling through mutation or amplification of genes encoding key components is one of the most frequent occurrences in human cancer.

The PI3K pathway is commonly activated in response to hormones and growth factors that act through cell surface receptors. Similarly to the MAPK kinase pathway RAS proteins also play an essential part of the PI3K pathway. The PI3K gene is one of the best characterized effectors of RAS. PI3Ks are lipid kinases that phosphorylate the inositol ring of phosphoinositide lipids, creating secondary messengers. These messengers propagate intracellular signalling through the regulation of the activation and the localisation of a number of target proteins including those that contain pleckstrin homology (PH) domains. Among the proteins which have PH domains there are two protein-serine kinases, PDK1 and AKT (also known as PKB). When AKT is activated, they phosphorylate numerous downstream substrates such as proapoptotic proteins BAD and caspase-3/7/9 that control survival [121]. There is a recent evidence that AKT promotes cell survival by indirectly activating NF-κB, which is considered to be an important pleiotropic transcription factor involved in the control of expression of various anti-apoptotic genes [122]. AKT also phosphorylates Mdm2 protein that antagonizes p53-mediated apoptosis. Phosphorylation of Tsc2 leads to the activation of rapamycin (mTOR)–containing protein complex mTORC1 that results in an increased protein synthesis by phosphorylation of eukaryotic initiation factor 4E and the ribosomal S6 protein [120].

Therefore, PI3-kinase pathway is a key regulator of cell survival. PI3K dependent AKT activation can be regulated through the tumor suppressor PTEN, which works essentially as the opposite of PI3K mentioned above. PTEN is a negative regulator of the PI3K pathway. PTEN regulates the level of the lipid phosphatidylinositol phosphate levels (PIP3) and its

inactivation results in accumulation of PIP3, AKT hiperphosphorylation and increased survival and division [123].

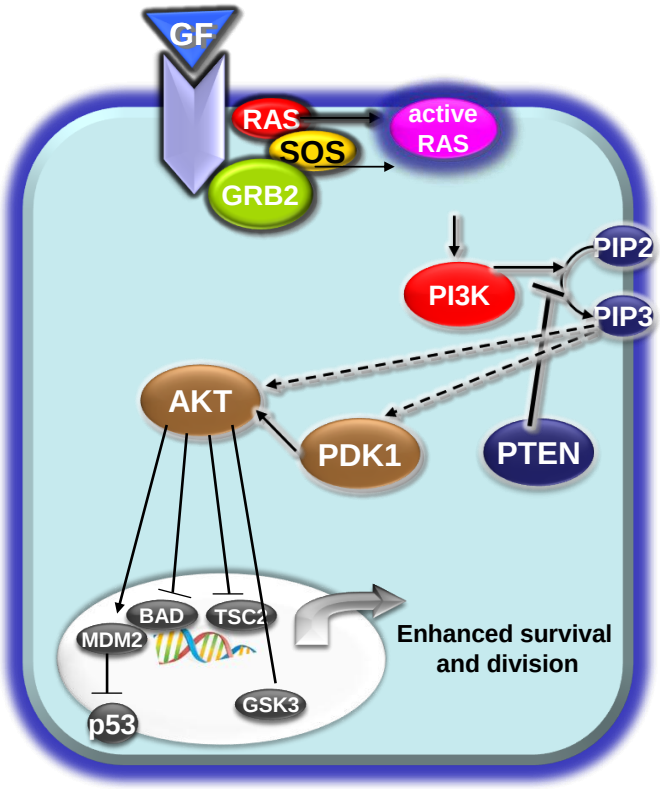

Figure 5. Simplified view of the PI3K pathway, with emphasis on components implicated in melanoma. (*J Clin Oncol*, 28(6):1075-1083) [123].Growth factor: **GF**; phosphatidylinositol (4,5)-bisphosphate: **PIP2**; phosphatidylinositol (3,4,5)-trisphosphate: **PIP3**; phosphoinositide-dependant kinase 1: **PDK1**.

Melanoma cells often show constitutive activation of the PI3K pathway due to increased PI3K and AKT expression or loss of PTEN gene function via point mutation or deletion. The first indication of involvement of the PI3K pathway in the progression of melanoma was the discovery of the frequent deletion of the PTEN tumorsuppressor gene. The PTEN gene is located at the chromosome 10q23.3. Cytogenetic and molecular genetic findings suggest that 10q deletion is a frequent and early event in the progression of malignant melanomas. The deletion was observed in approximately 30-50% of primary melanomas, the somatic mutation of PTEN occur in 10% of primary melanomas [124-127]. There is also frequent mechanism of PTEN inactivation typically through promoter hypermethylation [128]. It has also been reported that an another common mechanism behind the hyperactivation of PI3K pathway in melanoma development is the copy number increases of the long arm of chromosome 1 containing the AKT3 gene (located at the region of 1q44) [129]. Approximately 60% of melanoma tumors expressed elevated levels of Akt3 protein compared with normal human

melanocytes demonstrating a key role in melanoma development [130]. Recently, a low frequency activating mutation (E17K) in the PH domain of Akt3 has been identified in melanoma cell lines and 4% of primary tumors [131]. Moreover, the PI3Kα protein was found to be up-regulated [132]. An increase in tumor aggressiveness is observed in metastatic melanoma, which often correlates with the loss of PTEN or up-regulation of AKT3 [133].

Targeting PI3K signaling has significant clinical potential for inhibiting melanoma tumor development and components of this pathway present attractive targets for cancer therapeutics [134]. Several studies have indicated the potential use of inhibitors of the AKT signaling pathway (LY294002, wortmannin) for the chemosensitization of human carcinomas [135]. Others synthetic and naturally occurring small molecule inhibitors specifically inhibiting AKT activity have been developed and efficacy tested for inhibiting melanoma development in cultured cells and xenografted animal models [130, 136, 137]. For example an AKT inhibitor (BI-69A11) was demonstrated to effectively inhibit melanoma tumor growth [138].

1.8.3. Wnt pathway

Wnt signalling pathway is a complex system which affects numerous cellular functions in embryonic development, cell differentiation, cell polarity and cell homeostasis (Figure 6). The Wnt proteins are secreted glycoproteins that bind to their different receptors (LRP, FZ) and activate three protein cascades. 1) Molecules of the β catenin pathway reach the nucleus and activate target genes. This signalling is important in many developmental processes including the formation of neural crest-derived melanocytes. 2) The planar cell polarity pathway, which involves jun N-terminal kinase (JNK) and cytoskeletal rearrangements, and 3) The Wnt\Ca^{2+} pathway, that leads to release of intracellular Ca^{2+} [139]. Increased concentration of calcium activates Cdc42 (cell division control protein 42) through protein kinase C (PKC). Cdc42 regulates cell adhesion, migration, and tissue separation [140]. In the absence of WNT signalling, a comlex containing GSK3 phosphorylates β catenin, leading to degradation by ubiquitination.

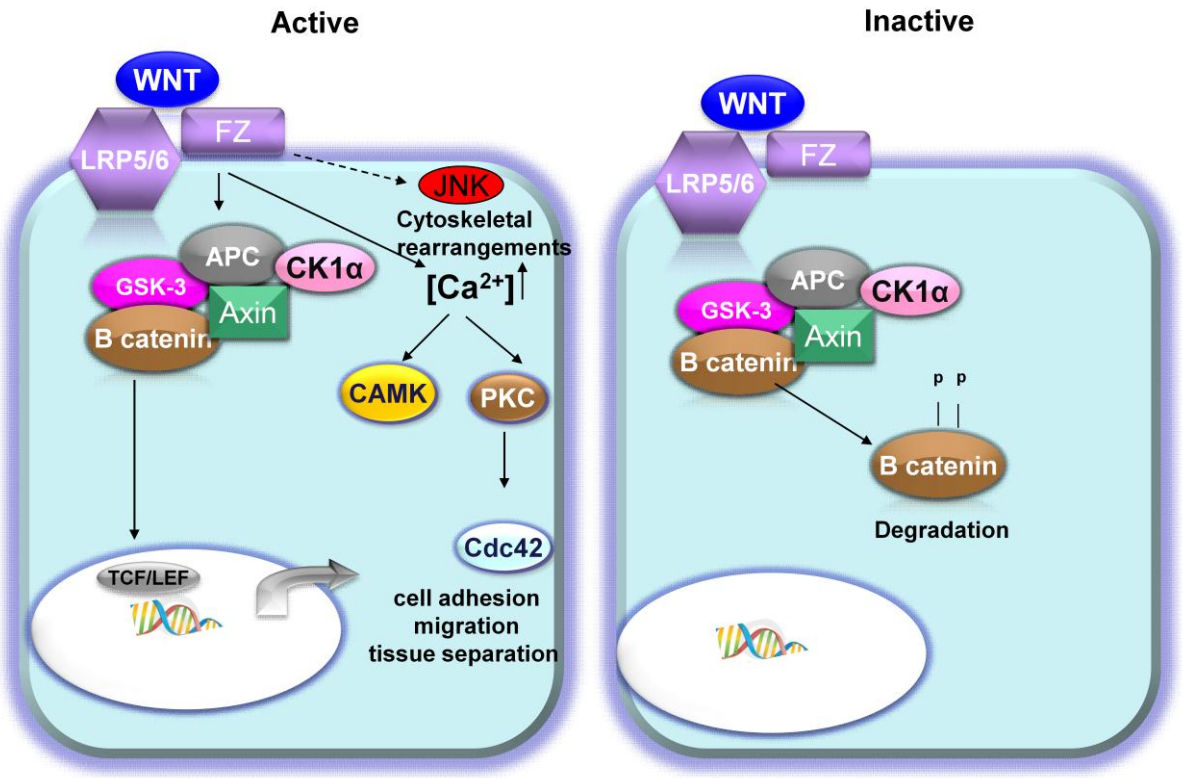

Figure 6. Simplified view of the WNT signalling cascade, with emphasis on components implicated in melanoma (*Journal of cell science* 2002, 115(Pt 21):3977-3978.) [139]. Ca2+/ calmodulin-dependent protein kinase: **CAMK**, c-Jun N-terminal kinases: **JNK**, Frizzled is a family of G protein-coupled receptor: **FZ**, The LDL receptor–related protein: **LRP**, cell division control protein 42: **Cdc42**, protein kinase C: **PKC**.

The molecular and cellular mechanisms involved in the proliferation and migration of melanoblasts during development of melanoma cells and during tumor progression are often closely related. Therefore it explains the important role of the Wnt pathway during melanoma progression that is constitutively activated in melanoma. Several components of the β catenin pathway are altered in melanoma tumors and cell lines, leading to activation of this signalling. Activation of this pathway leads to abnormally large amount of beta-catenin in the nucleus and in the cytoplasm. β catenin is found in about 30% of human melanoma nuclei, indicating a potentially specific role. β catenin can induce the activation of different genes including MYC or CCND1, BRN2 and melanocyte-specific genes such as MITF and DCT. The MITF and BRN2 genes encode transcription factors. MITF plays a critical role in melanocyte survival, proliferation and differentiation, while BRN2 is involved in melanoma proliferation [141]. It has been reported recently that specific WNT genes are overexpressed in human colon cancer and melanoma, further supporting the important role of WNT pathway in human carcinogenesis [142].

The blockade of this pathway by using specific inhibitory agents has been shown to suppress growth and invasion of melanoma cells. Previous findings also suggest that Wnt-2 monoclonal antibody may not only directly induce apoptosis in melanoma cells but its overexpression may also partially reverse chemotherapy-induced drug resistance [143]. Wnt inhibitory factor-1 (WIF-1) is a secreted antagonist of Wnt signalling. Moreover a recent study demonstrated that WIF-1 expression suppressed tumor growth in a xenogaft mouse model [144].

1.8.4. Notch pathway

Notch signalling pathway is a highly conserved system that affects the differentiation, proliferation, and apoptotic programs (Figure 7). It offers tools to control cell fates through local cell interactions. Most of the ligands of this pathway are transmembrane proteins. Therefore signaling is restricted to neighboring cells. This pathway plays an important role in the tissue communication development through the cell fate decision. The extracellular domain of the ligands, expressed on the cell surface such as Delta-like and Jagged ligands in human, interacts with the extracellular domain of the Notch receptor on an adjacent cell. As a result of receptor activation proteolytic cleavage events are promoted in the Notch receptor. The proteolytically cleaved intracellular domain of Notch receptor enters the nucleus and interacts with the DNA-binding proteins and directly modulates nuclear events [145].

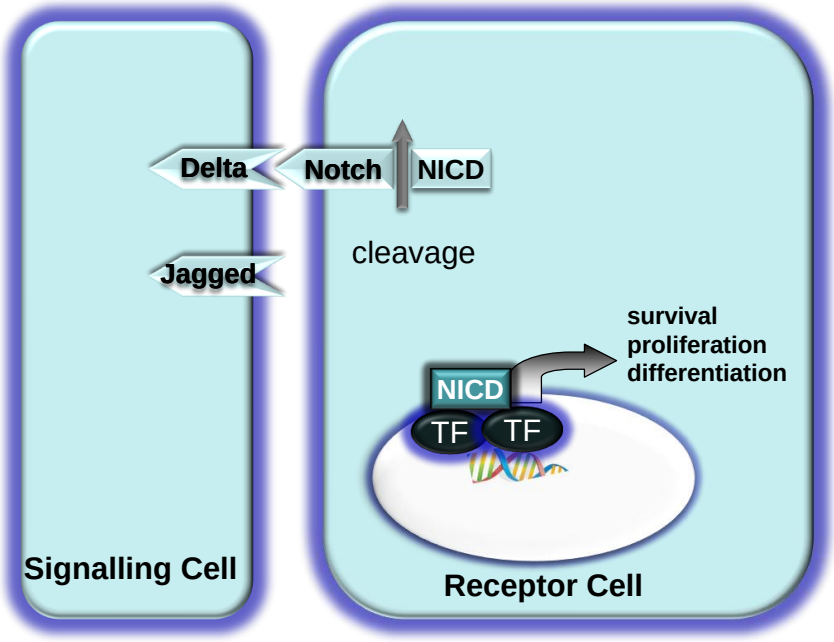

Figure 7. Simplified view of the Notch signaling cascade, with emphasis on components implicated in cancer development. Transcription factor: **TF**, intracellular domain of Notch receptor: **NICD**. The figure is based on the study of Artavanis et al. (*Science* 1999, 284(5415):770-776) [145].

Since this pathway has a key role in linking the control of epidermal differentiation and proliferation and in the keratinocyte-melanocyte interactions, recent findings imply that aberrant Notch signaling leads to the development of cutaneous melanoma. Microarray studies showed that Notch2 mRNA is overexpressed in melanoma cells compared to nevi and normal melanocyte [146]. Moreover constitutive activation of Notch1 signaling were found to drive the vertical growth phase (VGP) of primary melanoma toward a more aggressive phenotype [147]. It was also demonstrated that Notch activation represents an early event in melanocytic tumor growth and upregulation of Notch signaling could maintain melanoma progression [148]. The metastatic potential that Notch activation confers to primary melanoma cells must be, at least in part, mediated by the change in adhesion properties of melanoma cells [147]

Targeting the molecules of the Notch signalling pathway appears to be a promising therapeutic approach for the treatment of melanoma and perhaps the prevention of melanoma metastasis [149]. In a recent study Notch signalling was targeted by using a novel inhibitor of gamma secretase (RO4929097). The growth of human primary melanoma xenograft in mice was successfully decreased and inhibited the subsequent tumor formation in a serial xenotransplantation model [149]. However, an important question is still open whether therapeutically effective Notch inhibition can be accomplished *in vivo* without unacceptable toxicity. This is a common concern when manipulating key cell fate mediators. Systemic adverse effects might be avoided by 'smart' delivery strategies that use targeted local release of these agents.

1.8.5. The Hedgehog pathway

The Hedgehog (HH) pathway regulates cell differentiation and self-renewal in the developing embryo and is typically silenced in adult tissue. One out of the three HH pathway ligands (Desert-HH, Indian-HH, and Sonic-HH) binds to the transmembrane receptor PTCH1 to initiate pathway signalling (Figure 8). This event stops the suppression of SMO. SMO transduces the signal via COS2/FU complex and the SUFU. This process promotes the dissociation of the GLI1 transcription factor that leads its nuclear translocation and the activation of several target genes [150].

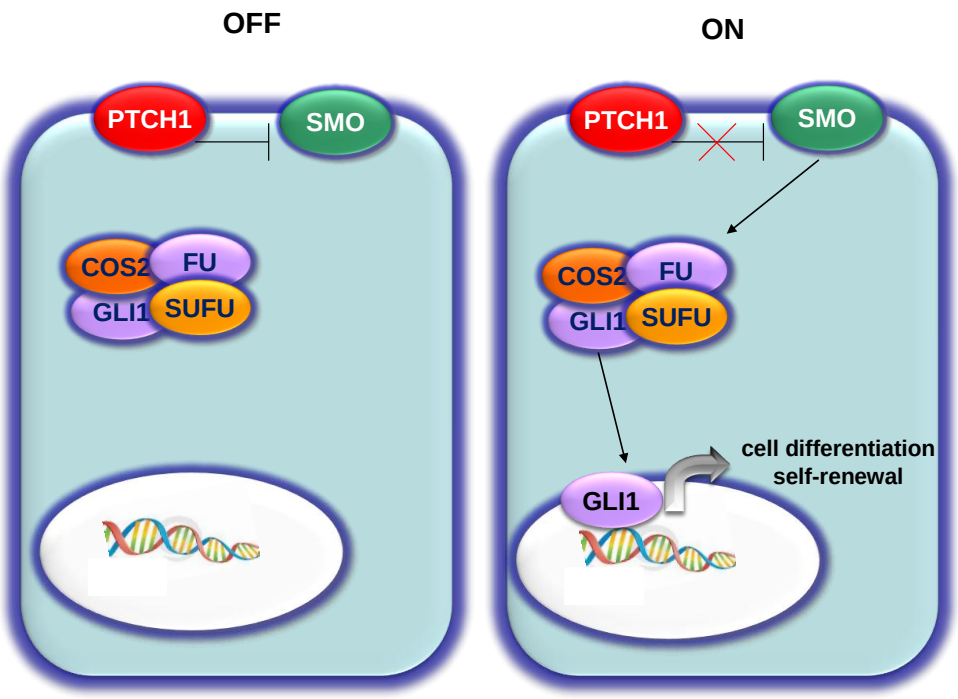

Figure 8. Simplified view of the HH signaling cascade, with emphasis on components implicated in cancer development. (*OncoTargets and therapy* 2012, 5:47-58) [150].

Suppressor of Fu: SUFU, Costal 2: COS2; transmembrane receptor Patched: PTCH, GLI family zinc finger 1: GLI1, smoothened, frizzled family receptor: SMO.

Increased transcription of HH target genes results in increased cell proliferation and survival, induction of stem cell markers [151]. Recent evidences also indicate that activation of the HH pathway plays an important role in several human cancers. The HH pathway activity in melanoma tumorigenesis was also revealed. GLI2 was found to be directly involved in driving melanoma invasion and metastasis. Melanoma cells with high GLI2 expression metastasized to bone more readily than cells with low GLI2 expression [152]. Moreover, they also proved that decreased GLI2 expression could have blocked bone metastasis of melanoma. Another study determined that GLI1 expression was correlated with tumor progression and metastasis of human melanomas [153].

Given that HH signalling is implicated in a wide range of malignancies, it is believed that HH pathway inhibitors may be promising drugs in clinical application. There are recent evidences that the first SMO protein antagonist cyclopamine delayed melanoma tumor growth in immunodeficient mice [154].

Aims

It is well known that activating mutations in BRAF and NRAS oncogenes are, so far, the most common single mutations detected in melanoma and the majority of benign nevi, but it is also clear that isolated mutations are not sufficient to initiate human melanoma in vivo. However the significance of BRAF and NRAS mutations in primary melanoma is still unclear. Therefore the major objectives of our study were the following:

I. to elucidate chromosomal regions that differs in copy number between BRAF, NRAS mutated primary melanomas ($BRAF^{mut}$, $NRAS^{mut}$) and tumors with wild type for both loci (WT)

II. to reveal chromosomal alterations that coexist more often in $BRAF^{mut}$ or WT melanomas

III. to explore a set of gene copy number alterations that has significant impacts on dysregulation of the MAPK pathway along with the BRAF mutation

IV. to investigate gene copy number alterations between and within different signalling pathways in genetically different melanoma subgroups

V. to develop a sensitive Q-PCR method for determining the amplification pattern of six candidate genes (TAOS1, FGF3, FGF19, FGF4, EMS1 and CCND1) that map to the 11q13 amplicon core

VI. to elucidate the combined incidence of the BRAF and NRAS mutation and the oncogenes located in the 11q13 amplicon core and their associations with clinicopathological parameters.

Materials and Methods

Tumor samples and DNA Isolation

The melanoma tissue samples were collected in the Department of Dermatology, Medical and Health Science Center, University of Debrecen (Debrecen, Hungary). The study was approved by the Regional and Institutional Ethics Committee, Medical and Health Science Center, University of Debrecen, and conducted according to its standard guideline (DEOEC RKEB/IKEB 2371-2005 and 2836-2008). Diagnoses of the tumors were carried out on formalin fixed paraffin embedded tissue sections using hematoxylin and eosin staining. Melanoma tumor staging was determined according to the new TNM staging system [28]. The distinction between tumor groups arising from chronically sun exposed sites or intermittently sun exposed site was based on the presence or absence of solar elastosis of the dermis surrounding the melanomas.

Gene copy number alterations of the 11q13 amplicon were analyzed in 68 primary and 6 metastatic melanomas by Q-PCR. Clinicopathological data of the primary tumors are listed in Table 1. Moreover, 47 primary tumors were subjected to extract DNA for array CGH analysis (Table 2). Thirty three primary melanoma tumors were analyzed using both methods.

Tumor DNA was extracted using the G-spin Genomic DNA Extraction Kit following the instructions of the manufacturer (Macherey-Nagel, Düren, Germany) [29]. NucleoSpin® Extract II kit (Macherey-Nagel) was used for the purification of DNA if it was needed. Only high quality DNA template was accepted with an absorbance ratio range between 1.79-1.9 (260nm/280nm) and 1.7- 2.5 (260nm/230nm) as measured by NanoDrop 1000 instrument (NanoDrop Technologies, Wilmington, Delaware USA). Control DNA was extracted from peripheral blood cells acquired from 8 different healthy individuals using the Nucleo Spin Blood mini kit according to the manufacturer's instructions (Macherey-Nagel). All DNA samples were stored at -20°C.

Table 2. Clinical and hystopathological parameters of primary melanomas analyzed in the array CGH study

	No. of tumors detected by	
Variables	**array CGH**	**Quantitative PCR**
All tumor	47	68
Tumor type [1]		
NM	19 (40.4 %)	26 (38.2%)
SSM	28 (59.6 %)	42 (61.7%)
Gender		
Male	24 (51.1%)	33 (48.5%)
Female	23 (49 %)	35 (51.4%)
Age (years)		
20-50	15 (31.9 %)	18 (26.4%)
>50	32 (68.1 %)	50 (73.5%)
Breslow thickness (mm) [2]		
<2.01	17 (36.2 %)	27 (39.7%)
2.01-4.00	9 (19.1 %)	13 (19.1)
>4.00	21 (44.7 %)	28 (41.1%)
Clark's level		
I, II, III	20 (42.6 %)	31 (45.5%)
IV, V	27 (57.4 %)	37 (54.4%)
Ulceration		
Absent	19 (40.4 %)	31 (45.6%)
Present	28 (59.6 %)	37 (54.4%)
Metastasis formation		
Nonmetastatic	20 (42.6 %)	25 (36.7%)
Metastatic	27 (57.4 %)	32 (47%)
BRAF^{mut} [3]		
Absent	26 (55.3 %)	43 (63.2%)
Present	19 (40.4 %)	25 (36.7%)
NA	2 (4.3 %)	
NRAS^{mut} [4]		
Absent	37 (78.7 %)	55 (80.8%)
Present	7 (14.9%)	13 (19.1%)
NA	3 (6.4 %)	-

[1] NM, Nodular Melanoma; SSM Superficial Spreading Melanoma
[2] Thickness categories based on the current melanoma staging system
[3] The distribution of *BRAF* codon 600 mutation
[4] The distribution of *NRAS* codon 61 mutation
NA: not available

Detection of BRAF and NRAS mutations

Analysis of mutations in the BRAF codon 600 and in the NRAS codon 61 was performed on LightCycler real time PCR System (Roche Diagnostics, GmbH, Mannheim, Germany) by melting curve analysis using fluorescent probes. All primers and probes were purchased from TIB Molbiol (Berlin, Germany) (Table 3). Amplification was performed in glass capillaries

using 50 ng of sample DNA in a 10 µL volume containing 1 µL 10X LightCycler FastStart DNA Master HybProbe (Roche Diagnostics, GmbH, Mannheim, Germany), 0.8 µL 25 mM $MgCl_2$, 0.75 µL DMSO, 1 µL (5 µM) forward and reverse primer, and 1 µL (2 µM) of the anchor and sensor hybridization probe.

TABLE 3. Sequences of oligonucleotides used for this study.

Gene	Forward Primer (5' ⟶ 3')	Reverse Primer (5' ⟶ 3')
GNS	TCCAACTTTGAGCCCTTCTT	CGTTCCATGGATGTTGAAGT
UBE2E1	GGTGGGAAGTATTGCCACTCA	GTGAAACCCCAATTTATGTAGCGTAT
CCND1	GCTCCTGGTGAACAAGCTCAA	TTGGAGAGGAAGTGTTCAATGAAA
TAOS1	TGCACGCACCTGTTTAAATTTTC	TTGGAGAGGAAGTGTTCAATGAAA
FGF3	GGGAACGCGAGTCCCTTTA	CCTTTTGTTGGCGAACCGT
FGF19	CGGATCTCCTCCTCGAAAGC	CCACTGTGGATTGCTCAGAGC
FGF4	CAACGCCTACGAGTCCTACA	AGGAAGTGGGTGACCTTCAT
EMS1	CAAGCTGAGGGAGAATGTCTT	TTGTTCCACACCAAATTTCC
BRAF V600	CTCTTCATAATGCTTGCTCTGATAGG	TAGTAACTCAGCAGCATCTCAGG
NRAS Q61	CACCCCCAGGATTCTTACAGA	GATGGCAAATACACAGAGGAAGC
Fluorescence probes	**Sensor (5'⟶ Fluoroscein- 3')**	**Anchor (5'-LCRed640 ⟶ Phosphate- 3')**
BRAF V600	AGCTACAGTGAAATCTCGATGGAG	GGTCCCATCAGTTTGAACAGTTGTCTGGA
NRAS Q61	ATACAGCTGGACAAGAAGAG	AGTGCCATGAGAGACCAATACATGAGGA

Underlined sequences correspond to *BRAF* codon 600 and *NRAS* codon 61, respectively.

The reaction was performed under the following condition: initial denaturation at 95°C for 10 minutes and 45 cycles of amplification consisting of denaturation at 95°C for 0 second, annealing at 52°C for 10 seconds and amplification at 72°C for 20 seconds. Melting curve analysis was done as follows: PCR products were denatured for 1 minute at 95°C then cooled down to 40°C for 1 minute and warmed up to 72°C (ramping at 0.1°C/second) with continuous fluorescence detection before by a final cooling step at 40°C for 30 seconds. The accuracy of the method was confirmed by direct sequencing (BIOM Kft., Gödöllő, Hungary) of PCR products that showed deviation from the wild type a genomic DNA melting peak (Figure 9).

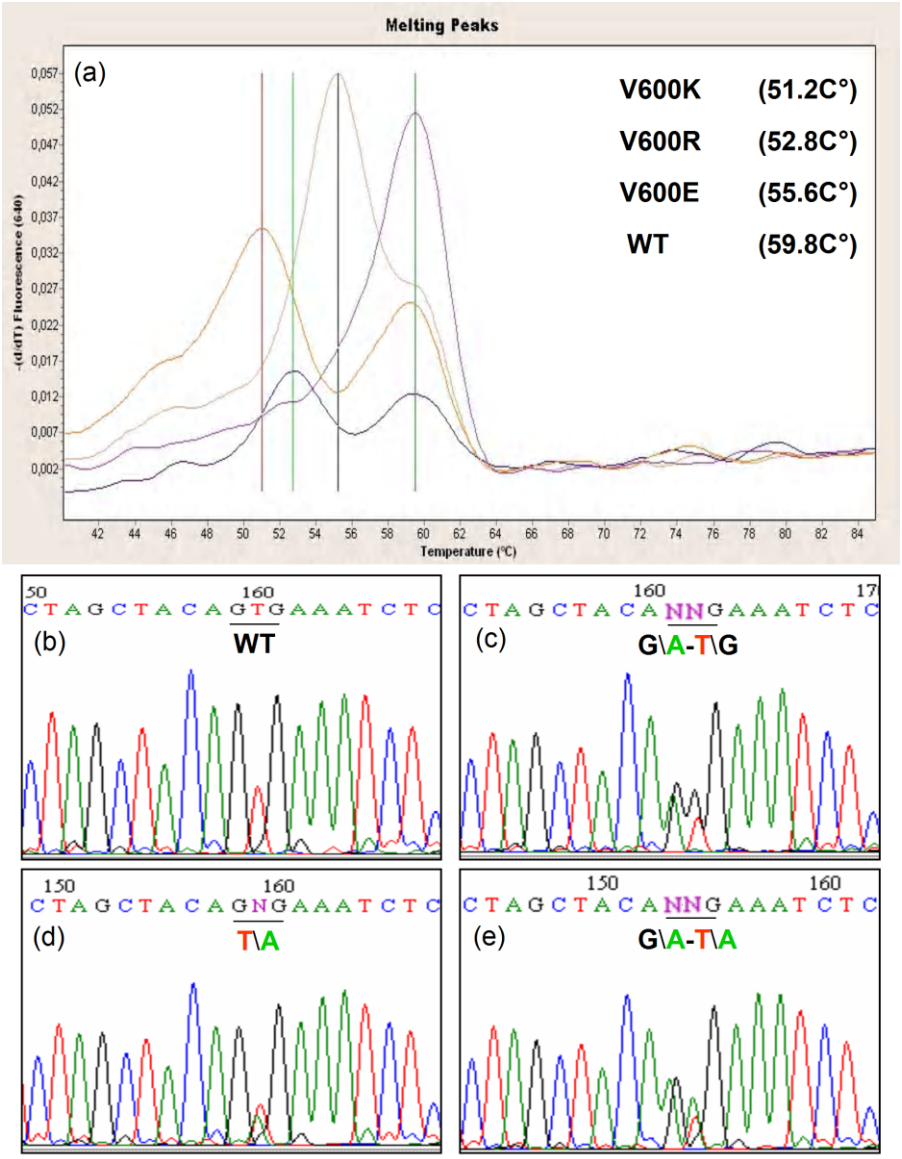

Figure 9: LightCycler melting curves and sequence traces of different BRAF types.
(a) Typical results of melting curve analysis, (b) BRAF WT sequence (codon 600 is underlined) (c) V600R mutation (GT1798-99AG double base pair substitution), (d) V600E mutation (T1799A base pair substitution), (e) V600K mutation (GT1798-99AA double base pair substitution).

Array CGH experiments

Array CGH experiments were performed on HumArray 3.1 in the University of California, San Francisco Cancer Center Array Core, as described before [155] (Figure 10). This array contains 2464 bacterial artificial chromosomes (BAC) and P1 clones, printed in triplicates and covering the genome at roughly 1.4 Mb resolution. One µg of tumor and normal reference DNA were labeled by random priming with fluorolink cy3-dUTP and cy5-dUTP, respectively. Then labelled DNA were mixed with 100 µg of Cot-1 DNA. Hybridization and

imaging setup was performed as described [100]. The acquired microarray images were analyzed by Spot and Sproc software [156]. DNA spots were automatically segmented, local background was subtracted, and the intensity ratio of the two dyes for each spot was calculated by $\log_2$ transformed modeling. Spots for which the $\log_2$ standard deviation of the triplicates was more than 0.2 were discarded

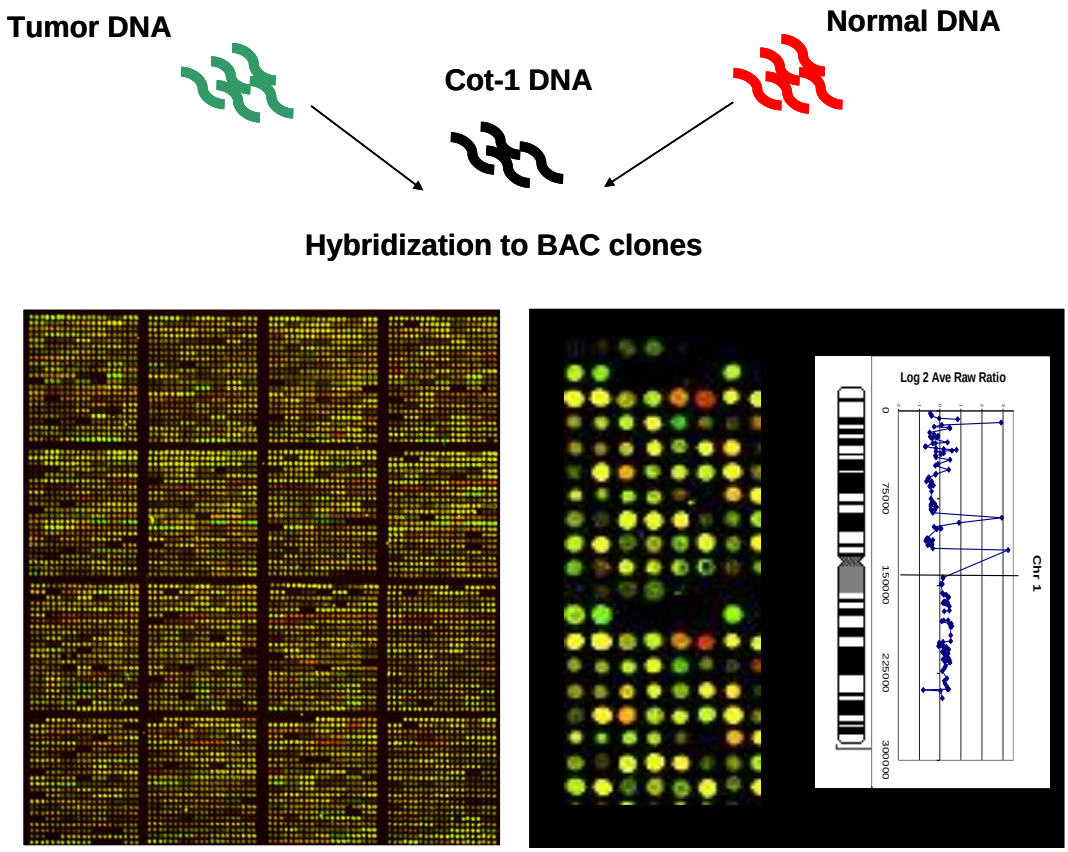

Figure 10. Schematic representation of array CGH

Differentially labeled test (tumor) and reference (normal) genomic DNAs along with unlabeled human Cot-1 DNA are cohybridized to BAC clones. Data along the arrayed BAC clones were extracted from scanned images and translated into log2 ratios of the Cy3 (green) labelled normal DNA and Cy5 (red) labelled tumor DNA signals, allowing us to measure DNA copy number changes in our samples. When the tumor DNA copy number is two, log2 (2/2) is 0. In the region where one copy is lost in the tumor, log2 (1/2) is -1.0. In the region of one copy gain in the tumor, log2 (3/2) is 0.58.

Array CGH data analysis

All BAC clones were mapped to the human genome using data provided by the UCSC genome browser site (http://genome.ucsc.edu/). From data processing, all X- and Y-chromosome clones were excluded. BAC clones, which are known to have genomic variants according to the Database of Genomic Variants (The Centre for Applied Genetics, Toronto,

Canada, http://projects.tcag.ca/variation/) were omitted. The $\log_2$ transformed data were subjected to copy-number change analyses for identification of regions of amplification and deletion. To determine gains and losses of each regions, the Analysis of Copy Errors (ACE) algorithm in CGH-Explorer software 3.2 was used with a False Discovery Rate (FDR) of <0.01 [157]. Previously, 11 different algorithms were compared which are most frequently used for analyzing array CGH data [158]. In this paper, they pointed out that some current implementations does not include any assessment of the statistical significance of the reported copy number changes, although quantitative statistics about the aberrations are critical in order to decide which region to pursue for further analysis. ACE is one of the two algorithms that incorporate FDR so far. The CGH Explorer was also used to obtain graphical illustrations of copy number alteration frequencies in primary melanomas.

For the subsequent identification of high level gains and homozygous deletions in array CGH data, ratio thresholds (>0.55 (> ~5 copies) and <-0.8, respectively) were used as described in previous studies [10]. Estimates of genome-wide aberration rates were made by simply calculating the proportion of BAC clones gained or lost in a specific tumor sample.

The two major objectives of our investigation were: 1) to identify BAC clones or regions that differ in copy number between tumor subgroups and 2) to examine correlations between these clones (which covers important onco- and/or tumorsuppressor genes) in order to define those that might act together in generating group differences.

To accomplish our first goal Fisher's exact test was applied to assess the probability of a possibly existing difference between the two groups. An FDR correction procedure was used to adjust for multiple comparisons and denote these resulting P values as adjusted P values [159]. In order to increase our power for identifying regional changes in copy number between tumor subgroups, log2 was averaged ratios over windows of five consecutive BAC clones and used a two-sample t statistic to compare the average log2 ratio for the tumor subgroups for each window. Then, an adjusted P value was calculated with a permutation based procedure of Westfall and Young [160].

The second aim, identification of the correlations between BAC clones in different tumor subgroups ($BRAF^{mut}$, WT) was achieved by calculating a standard Pearson correlation, which defines the magnitude and direction of the linear relationship between BAC clones to quantify whether those are changing in a concordant, discordant or unrelated manner. First a subset of BAC clones were chosen to distinguish the subgroups (see following for specific criteria) and then a pairwise correlation was computed for all of the BAC clones from the subset. BAC clones were selected if either the difference in the BAC's gain or loss percentages between the

tumor subgroups ($BRAF^{mut}$, $NRAS^{mut}$ and WT) was >40% or if its adjusted P value from the categorical or the windowed analysis was < 0.3 (similar to the approach that was applied by Loo *et al.* [161]). These selection criteria were chosen to include BAC clones that may truly differ between tumor subgroups but did not achieve statistical significance because of insufficient power. It should be emphasize that this procedure of selecting target BAC clones does not bias the correlation analysis because these selection criteria were based on comparison between tumor subgroups, whereas the correlations were calculated within each subgroup. All the cited P values were adjusted for multiple comparisons. The analyses were performed in the open source statistical computing environment "R" (http://www.r-project.org/).

Investigating the frequency of cross talks changed in primary melanomas

In cancer cells large-scale modifications of signaling pathways, especially in cross-talks, are prevalent [162]. The definition of cross-talk is the following: if two proteins belong to different pathways, then the signaling interaction between these two proteins is a cross-talk between their pathways. To identify cross-talks the SignaLink database was used (http://signalink.org/) which provides a precise mapping of signaling pathways and can also handle if a signaling protein belongs to more than one pathway [163]. To assess gene alterations in eight gene signaling networks (EGF/MAPK kinase (EGF), Insulin/IGF (IGF), TGF-ß (TGF), Wingless/WNT (WNT), Hedgehog (HH), JAK/STAT (JAK), Notch (Notch) and Nuclear Hormone Receptor (NHR)) we estimated the copy number changes of each of these pathway genes using the closest BAC clone within 2Mb. A signaling interaction was considered to be altered if the copy-number change of at least one of the participating genes was classified as a gain or loss by array CGH analysis, and then the average frequency of altered cross-talks was simply calculated within and between different pathways for a particular tumor subgroup.

Random Forest analysis

The Random Forest package [164, 165] of the R-statistical programming language (http://www.r-project.org/) was applied to calculate the random forest classification and importance measures on the array CGH data related to the MAPK pathway genes (clone number=138). The feature importance score derived from the random forest classifier was used to assess the association of a particular set of genes with positive BRAF mutations. The parameters were set as follows: ntree=5000 (number of trees) and mtry=11 (the number of randomly selected variables per branching of the tree). The most important 15 genes were listed and sorted by

their importance measures (Mean Decrease Gini and Mean Decrease Accuracy) over 1000 simulation runs and an automatic rerun was performed with a value of 3 for the mtry parameter using only those 15 variables that were most important in the original run. Cross-validation was preformed so the model was developed on the training set (60%) and validated on the test set (40%) of tumors.

Cluster analysis

Further evaluation of the genetic similarities between the primary tumors and altered regions that co-exist more often was performed by using unsupervised hierarchical clustering. For hierarchical clustering, the $\log_2$ transformed data were submitted for each BAC clone using the Pearson correlation as similarity metric and centroid linkage clustering with the Cluster 3.0 software [166]. Results were displayed using the TreeView program [167].

Primer design for Q-PCR analysis

The primers were designed for the genes GNS, UBE2E1, FGF3, FGF4, FGF19, EMS1 and TAOS1 using Primer Express 2.0.0 software (Applied Biosystems, Foster City, USA) and Primer3 (Whitehead Institute, Cambridge, USA) (http://biotools.idtdna.com/primerquest/) (Table 3). To avoid the secondary structures, the web-based MFOLD version 3.2 software (http://www.bioinfo.rpi.edu/applications/mfold/) was used [168]. The sequences of the primers for the CCND1 gene were downloaded from the RTPrimerDB database (http://medgen.ugent.be/rtprimerdb/) [169]. Primers were purchased from Biocenter Kft. (Biocenter Kft., Szeged, Hungary).

Real-time quantitative PCR analysis

Quantification of gene copy number was performed on 68 primary melanoma tissues and 6 melanoma metastases using Q-PCR. To quantify the relative amounts of the target genes, all located in the 11q13 amplicon core, two reference genes for normalization, GNS (12q14.3) and UBE2E1 (3p24.2) was selected. These reference genes have not yet been reported as having genetic abnormalities in melanomas analyzed by array CGH. To screen the copy number changes, two reference genes are needed to produce a robust, reliable and accurate quantification [170-173]. Reactions were carried out using an ABI Prism 7000 sequence detector (Applied Biosystems).

The amplification mixtures (25 µL) contained 1 µL template DNA (~10 ng/µL), 12.5 µL Power SYBR-Green PCR Master Mix (Applied Biosystems) and 100 nM of each primer for

TAOS1, FGF3, FGF19, UBE2E1 and FGF4, 200 nM of the primer for CCND1 and 300 nM of the primers for EMS1 and GNS. The reactions were performed under the following conditions: 10 minutes of polymerase activation at 95°C then 40 cycles at 95°C for 15 seconds and 60°C for 1 minute. Assay for each gene included: 1) no template control (in duplicate), 2) 10 ng of calibrator DNA (Applied Biosystems) (in triplicate) and 3) approximately 10 ng of tumor DNA (in triplicate). A melting curve analysis was run after the amplification was completed and consisted of a 20 minutes slow ramp from 60°C to 92°C using an ABI PRISM® 7000 Sequence Detection System (Applied Biosystems). The derivative melting curves showed single melting peaks, which confirmed the high Q-PCR specificity (absence of primer dimers and other nonspecific products). Our real-time quantitative PCR assay fulfills the MIQE (minimum information for publication of quantitative real-time PCR experiments) recommendation[174].

Real-time quantitative PCR data analysis

Quantification was performed using the Pfaffl method [175]. It requires the efficiency be known which needs to be determined with standard curves. In order to evaluate more accurately the PCR reaction efficiency, 5-point standard curves from three different four fold dilutions (ranging from 80ng to 0.3125ng) (in duplicate) were set up using melanoma cell line DNA (M24) for the different target genes and control DNA for the reference genes. To calculate the PCR amplification efficiency ($E = 10^{-1/slope} - 1$) the slope value has been calculated from the three separated standard curves for the target genes and reference genes as well. Only standard curves R^2 value >0.99 were accepted. Instead of interpolating unknown samples from a standard curve, the haploid copy number solely based on the observed C_T values has been calculated (eq.1)

$$Ratio = \frac{\left(1+E_{\text{target gene}}\right)^{-\Delta C_{T\ \text{target gene}}}}{\sqrt{\left(1+E_{\text{reference gene1}}\right)^{-\Delta C_{T\ \text{reference gene1}}} \times \left(1+E_{\text{reference gene2}}\right)^{-\Delta C_{T\ \text{reference gene2}}}}} \quad \text{(eq.1)}$$

Where

$E_{\text{target gene}}$ = efficiency of the PCR reaction for the target gene,

$E_{\text{reference gene}}$ = efficiency of the PCR reaction for the reference gene,

$\Delta C_{T\ \text{target gene}}$ = difference in threshold cycle value between test sample and calibrator sample for the target gene and

$\Delta C_{T\ \text{reference gene}}$ = difference in threshold cycle value between test sample and calibrator sample for reference gene.

The equation 2 was applied to calculate the standard error of the haploid copy number of the normalized target gene (SE target gene $_{(norm)}$).

$$\text{SE target gene}_{(norm)} = \text{target gene}_{(norm)} \times \sqrt{\left(\frac{\text{SE NF}_2}{\text{NF}_2}\right)^2 + \left(\frac{\text{SE RQ (target gene)}}{\text{RQ (target gene)}}\right)^2} \qquad \text{(eq.2)}$$

Where

RQ = sample quantity relative to calibrator sample.

$$\text{RQ}\left(\text{reference gene1}\right) = \left(1 + \text{E}_{\text{reference gene1}}\right)^{-\Delta C_{T\ \text{reference gene1}}}$$

$$\text{RQ}\left(\text{reference gene2}\right) = \left(1 + \text{E}_{\text{reference gene2}}\right)^{-\Delta C_{T\ \text{reference gene2}}}$$

$$\text{RQ}\left(\text{target gene}\right) = \left(1 + \text{E}_{\text{target gene}}\right)^{-\Delta C_{T\ \text{target gene}}}$$

The NF_2 is the normalization factor based on 2 reference (eq.3)

$$\text{NF}_2 = \sqrt{\text{RQ (reference gene1)} \times \text{RQ (reference gene 2)}} \qquad \text{(eq.3)}$$

The SE NF_2 is the standard error for this normalization factor (eq. 4.)

$$\text{SE NF}_2 = \text{NF}_2 \times \sqrt{\left(\frac{\text{SE RQ (reference gene1)}}{2 \times \text{RQ (reference gene1)}}\right)^2 + \left(\frac{\text{SE RQ (reference gene2)}}{2 \times \text{RQ (reference gene2)}}\right)^2} \qquad \text{(eq.4)}$$

Where

$$\text{SE RQ (reference gene)} = \text{E}^{\Delta C_{T\ \text{reference gene}}} \times \ln \text{E} \times \text{SE (reference gene } C_T)$$

$$\text{SE (reference gene } C_T) = \frac{SD}{\sqrt{m}} \text{ (m= number of measurements)}$$

$$\text{SE RQ (target gene)} = \text{E}^{\Delta C_{T\ \text{target gene}}} \times \ln \text{E} \times \text{SE (target gene } C_T)$$

$$\text{SE (target gene } C_T) = \frac{SD}{\sqrt{m}} \quad \text{(m=number of measurements)}$$

$$\text{target gene}_{(\text{norm})} = \frac{\text{RQ}\left(\text{target gene}\right)}{\text{NF}_2}$$

To determine whether copy numbers of the investigated genes are significantly different from the controls, a tolerance interval (TI) was set up for the relative gene copy number, using the mean SD of the ΔC_T values for target and reference genes in 12-14 normal DNA isolated form healthy individuals. The TI was the following equation: $TI = 2 \pm 2 \times SD\Delta C_T$. The TI ranged from 1.23 to 2.77 for CCND1 (n=14), 1.42-2.58 for TAOS1, 1.18-2.82 for FGF3, 1.1-2.9 for FGF4, 1.13-2.87 for FGF19 and 1.04-2.96 for EMS1 - (n=12). If the calculated diploid copy number of the normalized target gene ($2 \times (\text{target gene}_{(\text{norm})} \pm \text{SE target gene}_{(\text{norm})})$) exceeded the calculated upper limit the gene(s) in the tumors were considered to be amplified.

To check the validity of the genes used as reference genes (GNS/UBE2E1), the copy number ratio of the genes were analyzed in 14 normal control DNA samples and 74 tumor samples. The ratio for normal and tumor DNA were 0.92 (SD=0.072) and 0.96 (SD=0.205), respectively. The copy number ratios of the two reference genes in the normal and tumor DNA were similar (p=0.7236, Mann-Whitney test).

Results

Mutation frequencies of BRAF and NRAS oncogenes in primary melanomas

BRAF mutations at codon 600 were found in 25 out of 68 primary melanomas (36.8%) and in 2 out of 6 metastases. Eighteen (26.5%) primary and two metastatic lesions had BRAF exon 15, codon V600E mutations, which is a single-base T→A transition (T1799A), resulting in a valine to glutamine change and causing substitution with a negatively charged residue. Seven primary tumors (10.3%) with BRAFV600 mutations were double base pair tandem substitutions; five (7.4%) had a V600K (GT1798-99AA) mutation, causing a valine to lysine change in the amino acid; and two (2.9%) had a V600R tandem mutation (GT1798-99AG), causing a valine to arginine, both of which mutations resulted in a substitution of valine for a positively charged amino acid (Figure 9).

NRAS mutations at codon 61 were found in 13 out of 68 primary melanomas (19.1%) and in

2 out of 6 metastases. The two most frequent mutations observed were a CAA to AAA transversion, which occurred in seven primary lesions (10.3%) and two metastases (resulting in a Q61K change) and a CAA to CGA transition, which occurred in five primary tumors (7.4%) (resulting in a Q61R change). A CAA to TTA tandem mutation was observed in one lesion (1.5%) (resulting in a Q61L change). Furthermore, 55.8% of primary melanomas and 3 metastases had either BRAF or NRAS mutations, but both mutations were never simultaneously present.

Paired primary and metastatic tumor were available for the analysis in four cases. In three out of the four cases we found mutations in the primary tumors (one carrying a BRAFV600E mutation, two harboring a NRASQ61K mutation) and also in the corresponding metastatic lesions (data not shown).

NRAS codon 61 mutations were significantly more frequent in tumors originating from chronically sun-exposed sites (p=0.005) (Table 1). The molecular analysis of the types of mutations we found in the NRAS gene may provide some explanation for this pattern. UV radiation in sunlight damages DNA, forming predominantly cyclobutane dimers or 6-4 pyrimidine pyrimidone lesions at adjacent pyrimidines (TT, TC, CC, or CT). The strand opposite the NRAS codon 61 (CAA) contains a TT sequence, so this site is a prime candidate for UV damage. In a study where UV induced mutagenesis were detailed investigated in Escherichia coli they found that at the TT site the substitutions that were predominately recovered were the T to C transitions and the T to A transversions[176]. T to C transition one of the most common mutation that we found in NRAS codon 61 (CAA to CGA transition) is typical of UV exposure.

Frequent chromosomal alterations in 47 primary cutaneous melanoma cancer samples identified by array CGH

Tumor DNAs from 47 frozen tissue primary melanoma samples were analyzed with array CGH (see Table 2 for more details). To identify overall trends across all of the tumors we plotted the frequency of tumors showing gain or loss for each BAC clones across the genome (Figure 11) and listed the high frequency (>30% of tumors) of regional gains (>5Mb) and losses in Table 4.

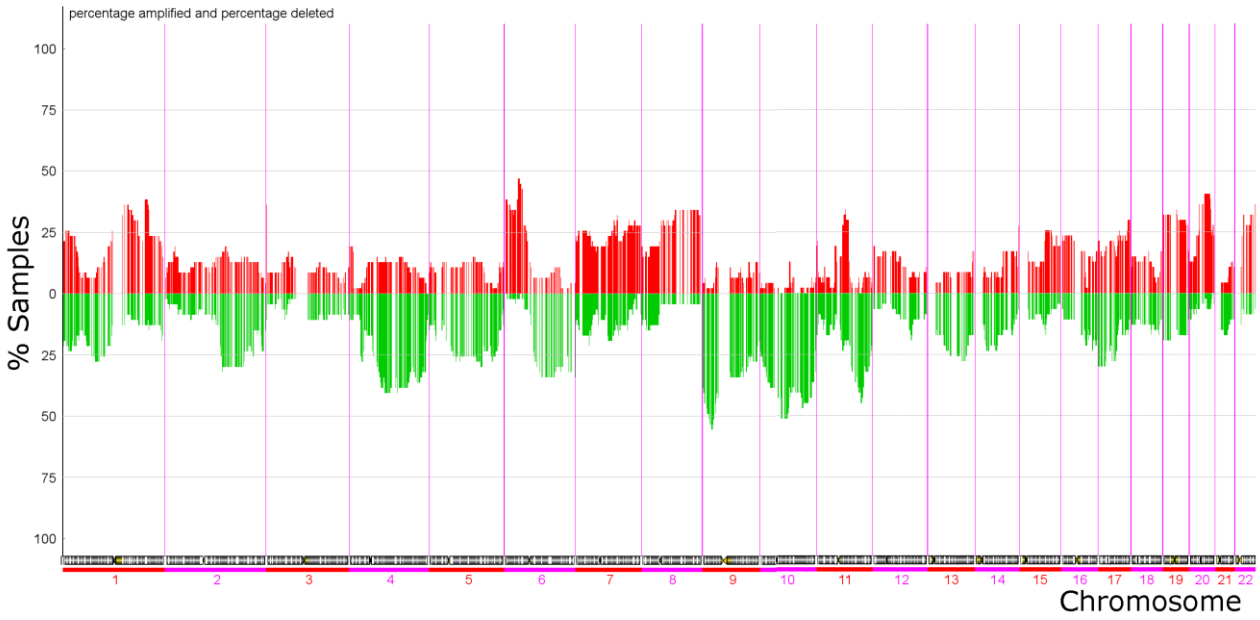

Figure 11. Overall frequency of BAC copy number gain and loss for 47 primary melanomas. The percentage of the 47 tumors showing gain (red; above 0) or loss (green; below 0) of DNA represented by each of the 2379 BAC is plotted against the corresponding genomic position of the BAC clone.

TABLE 4. High frequency (>30%) of regional (> 5 MB) gains and losses in 47 primary melanomas.

Chromosome location	Event	Number of BAC clones
1p36.31-p36.21	Gain	7
1q21.1 - 1q25.3	Gain	24
1q31.3 - 1q32.1	Gain	11
6p25.3- 6p12.3	Gain	43
7q31.2- 7q31.33	Gain	11
8q11.21- 8q12.3	Gain	20
8q21.11 - 8q24.3	Gain	57
11q13.1 - 11q13.4	Gain	29
15q22.2- 15q25.1	Gain	20
17q25.1 - 17q25.3	Gain	17
19p13.3 - 19q13.42	Gain	36
20p11.21 - 20q13.2	Gain	44
22q11.21 - 22q13.32	Gain	16
1p36.22 - 1p35.2	Loss	15
2q22.1- 2q32.2	Loss	49
4q13.3 - q35.1	Loss	107
5q22.3 - 5q23.2	Loss	8
6q13 - 6q27	Loss	37
9p24.3 - 9q32	Loss	102
10p15.3 - 10q26.3	Loss	130
11q14.1 - 11q24.2	Loss	51
13q14.3 - 13q31.3	Loss	20
17p13.3 - 17q21.32	Loss	46

Chromosomal regions that differs in copy number between BRAF^{mut}, NRAS^{mut} and WT primary melanomas

We were able to successfully identify the mutation status for BRAF and NRAS oncogenes (BRAF^{mut} or BRAF^{wt}, NRAS^{mut} or NRAS^{wt}) for 44 out of 47 primary tumors selected for array CGH analysis (Table 2). Tumors were classified into three groups a: 1) BRAF^{mut} primary melanoma (n=19); 2) NRAS^{mut} primary melanoma (n=7); WT (wild type for both loci) primary melanoma (n=18).

First the gain and loss frequencies in these mutation groups (BRAF^{mut}, NRAS^{mut}, WT) were compared and the average frequency of copy number changes was observed to be higher in BRAF^{mut} tumors than in WT tissues. (Mann-Whitney test; p=0.04 and p=0.01, for gains and losses, respectively). However, no other differences were found in genome wide aberration rates between these groups (Figure 12).

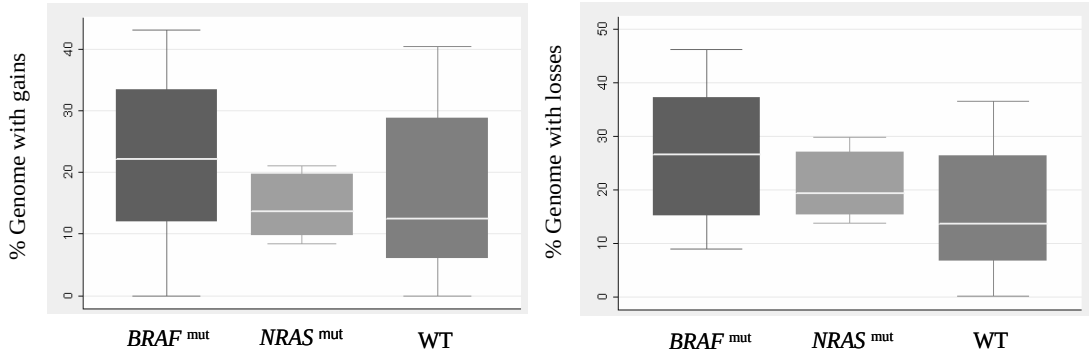

Figure 12. Differences in the number of alterations among the three mutation groups

The box plots indicate significant differences in the gain (Panel A) and loss (Panel B) frequencies among BRAF^{mut} and WT tumor tissues (Mann-Whitney test; p=0.0433 and p=0.0122, for gains and losses, respectively).

The frequency patterns of copy number changes for each group across the entire genome are shown in Figure 13. Four different methods were selected to identify BAC clones or groups of BAC clones that showed more frequent loss or gain in one tumor subgroup than another: 1) measurement of difference in frequency of gain or loss between subgroups were higher than 40%; 2) determination of significant differences in copy number changes of individual BAC clones between subgroups with Fisher's exact test; 3) determination of statistical difference between windows of five BAC clones with two-sample t statistic; and 4) characterization of high-level loss and gain in more than 20% of tumors in each subtype.

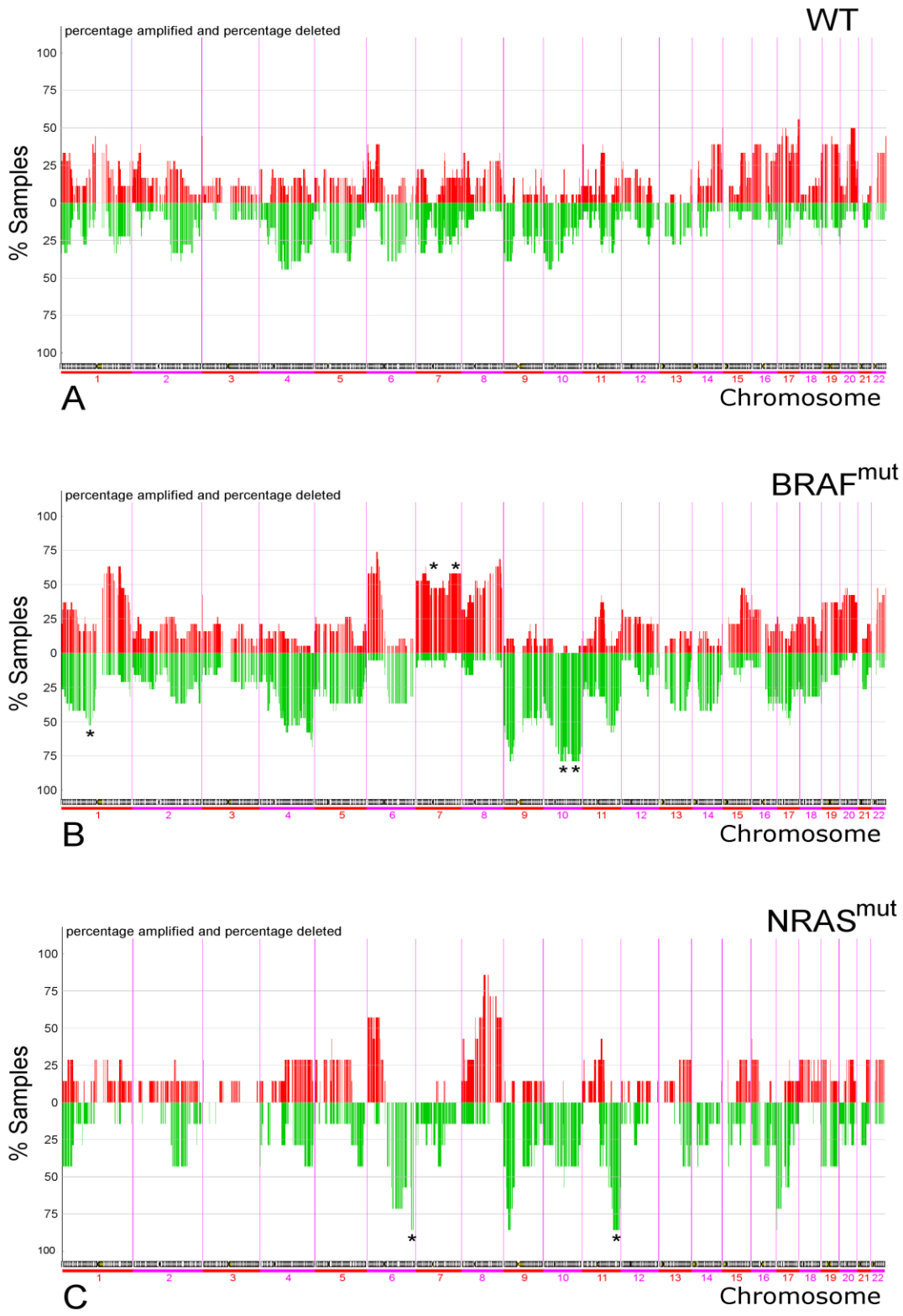

Figure 13. Frequency plots of copy number gain and loss in subgroups of primary melanomas. The percentage of copy number gain (red; above 0) and loss (green; below 0) were calculated for A) WT (n=18), B) $BRAF^{mut}$ (n=19) and C) $NRAS^{mut}$ (n=7) tumor tissues. (*) indicates regions significantly altered (adjusted P value<0.05) (or close to; adjusted P value<0.1) between mutation subgroups.

TABLE 5. Chromosomal loci that showed more frequent (more than 40%) gain or loss in one tumor subtype than another (BRAF ^{mut}, NRAS ^{mut}, WT).

BRAF^{mut} vs. NRAS^{mut}			
Chromosome location	**Event**	**Number of BAC clones [1]**	**Association**
1q23.2 - 1q25.2	Gain	16	BRAF^{mut}
7 chr	Gain	191	BRAF^{mut}
20q13.32	Gain	1	BRAF^{mut}
1p34.2 - 1p33	Loss	3	BRAF^{mut}
1p13.2	Loss	5	BRAF^{mut}
4q13.3	Loss	3	BRAF ^{mut}
4q22.1 - 4q25	Loss	3	BRAF ^{mut}
10q21.3 - 10q22.1	Loss	2	BRAF^{mut}
10q26.13 - 10q26.3	Loss	15	BRAF^{mut}
6q25.3 - 6q27	Loss	4	NRAS^{mut}
11q23.3 - 11q25	Loss	21	NRAS^{mut}
17p13.3	Loss	2	NRAS^{mut}
BRAF^{mut} vs. WT			
Chromosome location	**Event**	**Number of BAC clones [1]**	**Association**
1q24.1 - q24.3	Gain	4	BRAF^{mut}
1q25.3 - 1q31.2	Gain	4	BRAF^{mut}
6p22.3	Gain	7	BRAF^{mut}
7p22	Gain	11	BRAF^{mut}
7p21.3 – 7p21.1	Gain	3	BRAF^{mut}
7p15.3 – 7q36.3	Gain	128	BRAF^{mut}
8q11.11 - 8q11.22	Gain	4	BRAF^{mut}
8q24.11 - 8q24.3	Gain	31	BRAF^{mut}
1p33 – 1p32.3	Loss	3	BRAF^{mut}
9p21.1 - 9p13.3	Loss	6	BRAF^{mut}
9p13.2	Loss	1	BRAF^{mut}
10q11.21 – 10q26.3	Loss	93	BRAF^{mut}
11q22.1	Loss	1	BRAF^{mut}
11q23.1 – 11q23.2	Loss	6	BRAF^{mut}
11q14.2-11q23.3	Loss	15	BRAF^{mut}
NRAS^{mut} vs. WT			
Chromosome location		**Number of BAC clones [1]**	**Association**
8q12.2-8q21.11	Gain	14	NRAS^{mut}
8q24.23 - 8q24.3	Gain	3	NRAS^{mut}
6q22.31	Loss	2	NRAS^{mut}
6q25.2 - 6q27	Loss	6	NRAS^{mut}
9p22.2 - 9p21.3	Loss	5	NRAS^{mut}
11q21 - 11q25	Loss	38	NRAS^{mut}
17p13.3 - 17p11.2	Loss	30	NRAS^{mut}
17q12 – 17q21.2	Loss	15	NRAS^{mut}
4q23 – 4q25	Loss	4	WT
17p11.2	Gain	4	WT
17q24.3 – 17q25.3	Gain	15	WT

[1] Number of BAC clones altered in the region

In Table 5 those distinct chromosomal were listed that showed more frequent gains and losses (>40%) in one tumor subgroup than in another. Alterations exclusively associated with $BRAF^{mut}$ were the gain of chromosome 7 and 1q23-q25 and losses on the long arm of chromosome 10. Losses of the 6q25.3-q27, 11q23.3-q25 and 17p13.3 loci were the most common DNA alterations in $NRAS^{mut}$ tumor samples. Loss of the 9p region and gain of 8q were more frequent in melanomas with $BRAF^{mut}$ or $NRAS^{mut}$. Primary melanoma without *BRAF* or *NRAS* mutations was primarily characterized by amplification on the 17q24-17q25 and deletions on the 4q23-q25 chromosomal regions.

Using Fisher's exact test to compare the frequency of gain and loss of individual BAC clones between $BRAF^{mut}$ and WT tumor subgroups, we found that the loss of 45 clones from the 10q23.3-10q26.3 region were mainly associated with $BRAF^{mut}$ melanoma (adjusted p values < 0.05). Using slightly less conservative level of significance (adjusted $p<0.1$), as it was applied by Loo *et al.* [161], additional 73 BAC clones were indentified at the following locations: gains in 7p14.2 - 7q11.22 and 7q36.3 and losses in 1p33 and 10q21.1-10q23.31, which were found to be more frequent in $BRAF^{mut}$ than in WT tumors. Moreover, 29 BAC clones exhibited differences between $NRAS^{mut}$ and WT tumor subgroups. Loss in 6q25.2-6q25.3 and 11q23.1-11q25 were mainly seen in tumors with $NRAS^{mut}$, but none of these alterations were commonly seen in WT tumors. Asterisks on Figure 13 indicate the location of the BAC clones showing differences between these primary melanoma subgroups with this test. Our data shows, that these BAC clones achieving a level of significance with Fisher's exact test are often part of a larger region that differ in frequency of gain or loss between these tumor subtypes.

To increase our power in identifying copy number gains and losses larger than those identified by single BAC clones, a two sample t statistic was applied to compare a sliding window of five consecutive BAC clones in the tumor subgroups. With this test, differences between $NRAS^{mut}$ and WT tumor subgroups for BACs were bserved at the following locations: 11q23.2, 11q24.1-11q24.2, 11q25. There was also a suggestive evidence of differences between $BRAF^{mut}$ and WT tumor subgroups in 7q11.22, 7q11.23, 7q21.11, 10q11.23, 10q23.1, 10q23.1, 10q23.33-10q24.33 and 14q24.3.

To further characterize genomic differences between tumor subgroups, we also compared the frequency with which particular BAC clones showed high level amplifications and homozygous deletions exceeding the upper or lower thresholds ($\log_2$ ratio ≥ 0.55 or ≤ -0.8, respectively). BAC clones showing such alterations in at least 20% of the tumors in a subgroup were listed in Table 6. Frequent homozygous deletion was seen in both $BRAF^{mut}$

and WT melanomas in the 17q21.32 region harboring the HOXB3-9 gene cluster, which members are associated with many malignant tumors [177]. Homozygous deletion of the CDKN2A (9p21.3) gene was found only in 8.5% of tumors (4/47).

Table 6. The list of regions where the most common high-level amplification and homozygous deletions were observed

Chromosome location	Event	Association[1]
6p22.3	high-level amplification	$BRAF^{mut}$
7p21.3	high-level amplification	$BRAF^{mut}$
7p21.1	high-level amplification	$BRAF^{mut}$
7p15.3	high-level amplification	$BRAF^{mut}$
7p14.3	high-level amplification	$BRAF^{mut}$
7p14.1	high-level amplification	$BRAF^{mut}$
7p13	high-level amplification	$BRAF^{mut}$
7p12.3	high-level amplification	$BRAF^{mut}$
7p12.1	high-level amplification	$BRAF^{mut}$
7q31.2	high-level amplification	$BRAF^{mut}$
7q32.2	high-level amplification	$BRAF^{mut}$
7q35-q36.3	high-level amplification	$BRAF^{mut}$
8q24.13	high-level amplification	$BRAF^{mut}$
17q21.32	homozygous deletion	$BRAF^{mut}$ and WT
6p22.3	high-level amplification	$NRAS^{mut}$
6p21.31	high-level amplification	$NRAS^{mut}$
6p12.1	high-level amplification	$NRAS^{mut}$
13q21.33-13q22.1	high-level amplification	$NRAS^{mut}$
13q31.3-13q32.1	high-level amplification	$NRAS^{mut}$
13q33.1	high-level amplification	$NRAS^{mut}$
13q33.3	high-level amplification	$NRAS^{mut}$

[1] It was considered to be associated with a tumor subtype if at least 20% of primary melanomas in that particular subgroup showed this genetic alteration.

Correlation of gain or loss changes in $BRAF^{mut}$ and WT primary melanomas

Pairwise correlation analysis of the subset of $BRAF^{mut}$ and WT tumors (including 519 and 167 BAC clones, respectively; these clones exhibited more frequent loss or gain in these tumor subgroups) revealed chromosomal alterations that coexist more often together in these groups of tumors. The heat maps of Figure 14 show regions of positive (change in same direction: green) and negative (change in opposite direction: red) correlations between certain regions. The relatively large regions with strong positive or negative correlations (correlation coefficient >0.7 or <-0.7, repsectively) were found in WT tumors and $BRAF^{mut}$ melanoma. These are listed in Table 7.

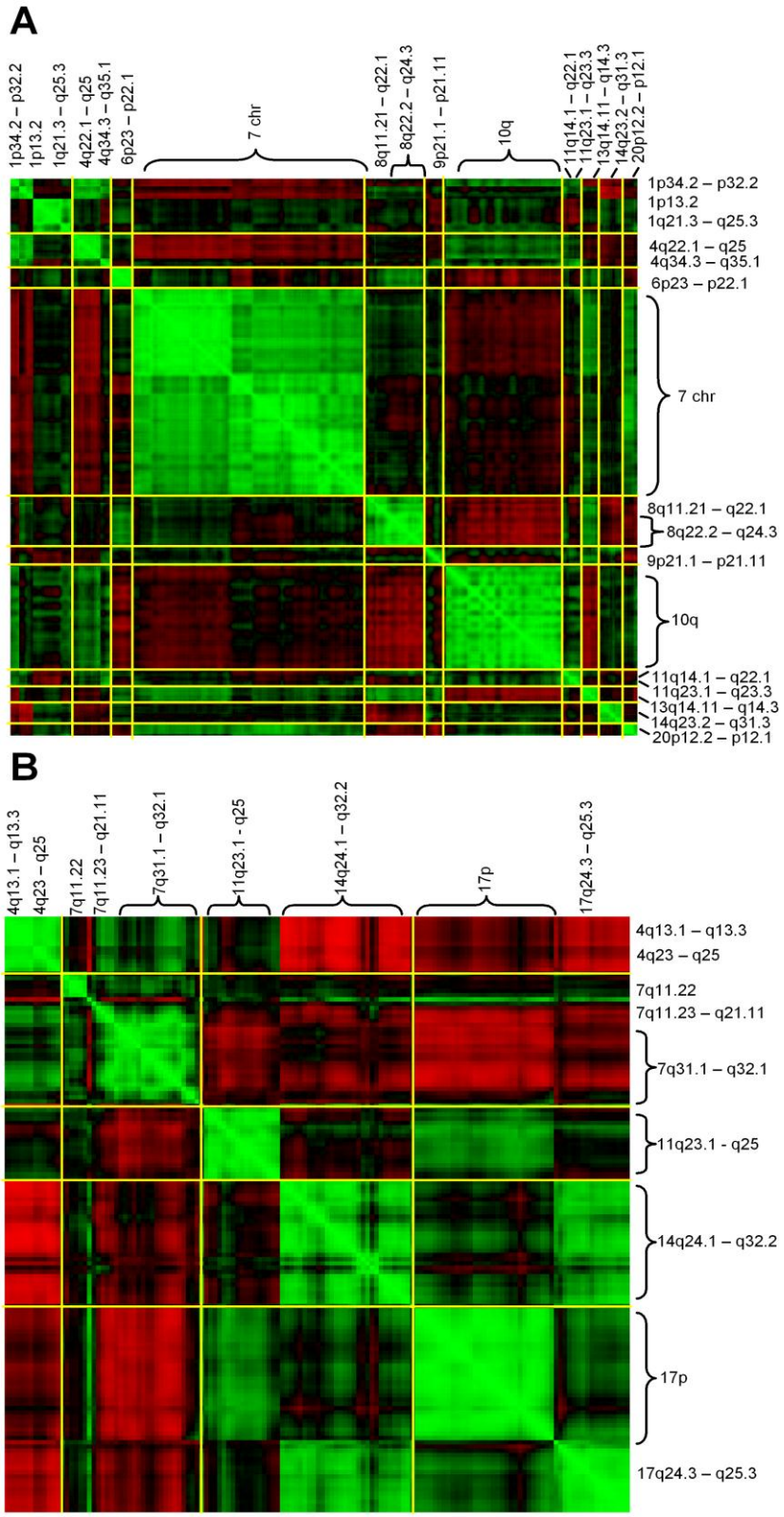

Figure 14. Correlation matrix of copy number changes for BRAF^{mut} and WT primary melanomas. The heat maps show positive (change in same direction; green) and negative (change in opposite direction; red) correlation between loss or gain of individual BAC clones for the 19 BRAF^{mut} (A) and 18 WT (B) tumors. The 519 or 167 BACs clones that showed frequent change in BRAF^{mut} or WT tumors are shown in genome order. Chromosomal band information is labeled.

Table 7. Paired genetic alterations at different genomic regions showing strong positive or negative correlation in BRAF^{mut} or in WT primary melanomas

BRAF^{mut} primary melanomas			
A) Chromosome location	**A) Event**	**B) Chromosome location**	**B) Event**
1p34.2-1p32.2	loss	4q22.1 - 4q25	loss
1p13.2	loss	4q22.1 - 4q24	loss
4q34.3 – q35.1	loss	11q23.2-q23.3	loss
7q21.11-q31.1	gain	20p12.2-p12.1	gain
WT primary melanomas			
A) Chromosome location	**A) Event**	**B) Chromosome location**	**B) Event**
4q13.1 - q13.3	loss	14q24.1 - q32.2	gain
4q13.1 - q13.3	loss	17q24.3 - q25.3	gain
4q23-q25	loss	14q24.1 - q32.2	gain
4q25	loss	17q24.3 - q25.3	gain
7q11.23 - q21.11	loss	17p	gain
7q31.1- q31.2	loss	17p	gain
7q31.31 - 7q31.32	loss	17p	gain
14q24.1 - q32.2	gain	17q25.1 - q25.3	gain

Cluster analysis of array CGH profiles

Because chromosome 10q loss was a frequent event in melanomas with BRAF^{mut} a detailed cluster analysis was performed of 10q, which revealed three clusters (A, B and C) with different genomic profiles. Cluster A and B mainly included advanced stage lesions (IV-V Clark's level, p=0.032) and was associated with losses of these regions involving the PTEN (10q23.3) locus. Tumors carrying BRAF^{mut} grouped mainly into cluster A (p=0.013) and had large deleted regions of chromosome 10q (Figure 15).

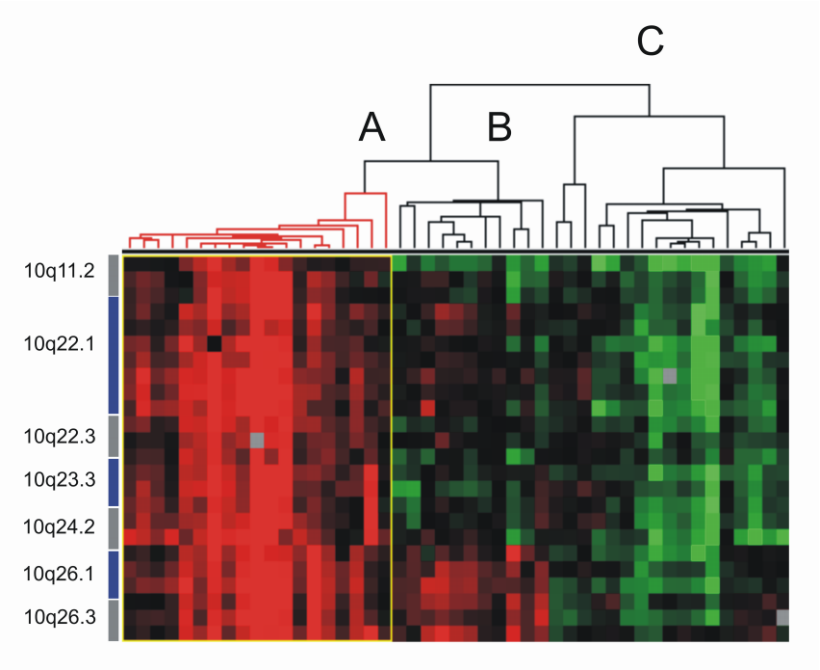

Figure 15. Cluster analysis of commonly altered regions at the chromosome 10q arm. Each column represents one case and each row represents one BAC clone. Three separate clusters are indicated (Cluster A, B and C). Cluster A and B mainly include patients with IV-V Clark's level (Cluster A and B versus C; p=0.032) involving the PTEN (10q23.3) locus. Tumors carrying BRAF mutation frequently occurred in cluster A at a significantly higher rate (Cluster A versus B and C; p=0.013). Green, red and black indicate higher, lower or no gene copy-number alterations, respectively. The color scale ranges from saturated red for log2 ratio -0.5 and to saturated green for log2 ratio 0.5. Gray represents missing data.

Identification of gene signature associated with the BRAF mutation in the EGF/MAPK pathway

Because the BRAF oncogene is one of the key activators of the EGF/MAPK pathway, we performed a focused analysis of this signaling pathway to investigate whether there are any gene signatures in this pathway that are related to the BRAF mutation. We estimated the copy number changes of each of these pathway genes using the closest BAC clone within 2 Mb. Using the random forest classifier among the EGF/MAPK pathway genes, we identified a signature of 15 genes that was highly predictive for a BRAF-positive mutation status (see Figure 16 for more details). A cross-validation test was carried out for each set of genes to evaluate the accuracy measures of the Random Forest model (Table 8).

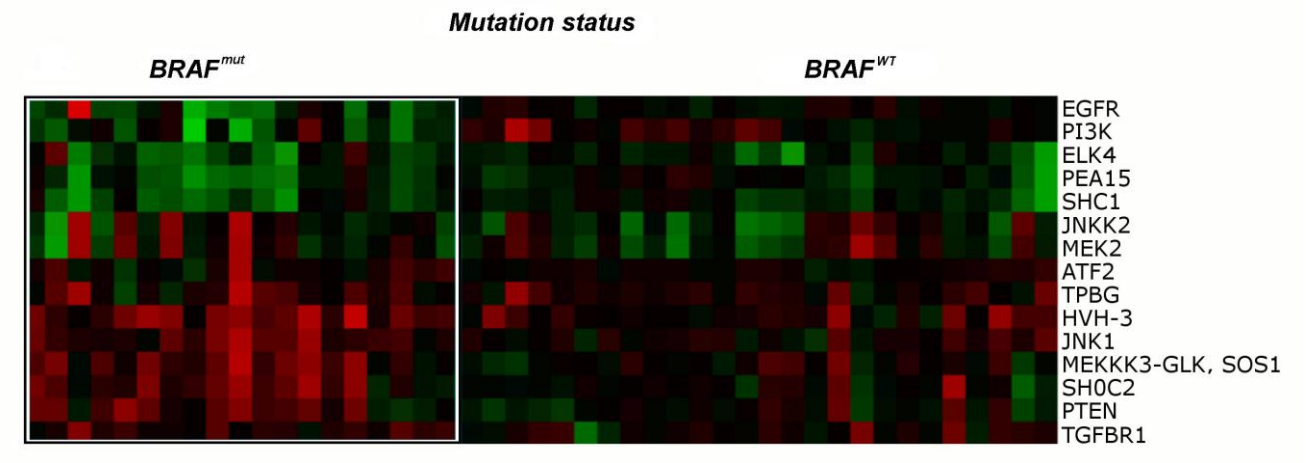

Figure 16. The heat map of the $BRAF^{mut}$ -and $BRAF^{wt}$ group for the 15 signature-genes determined by Random Forest. Green and red indicate higher or lower gene copy number, respectively. The different tumor groups are separated by white-colored line. The color scale ranges from saturated red for log2 ratio -0.5 and to saturated green for log2 ratio 0.5.

Table 8. Accuracy measures of Random Forest analysis

Mutation status	Accuracy	Sensitivity	Specificity
BRAF mutation	87.5%	77.8%	70.0%

Frequent changes of signaling cross-talks in primary melanomas harboring BRAF mutation

In this study another objective was to investigate the frequency of copy number changes of the signaling interactions between and within 8 tumor regulatory pathways (Mitogen Activated Protein Kinase pathway: EGF, Hedgehog pathway: HH, : Insulin-like Growth Factor pathway: IGF, Janus Activating Kinase pathway: JAK, Nuclear Hormone Receptor: NHR, Notch pathway: NOTCH, Transforming Growth Factor patway: TGF, Wingless pathway: WNT) in primary melanoma subgroups with different BRAF genotypes ($BRAF^{mut}$: tumors harboring BRAF mutation; $BRAF^{wt}$: tumors without BRAF mutation which also includes tumors with NRAS mutation). Results of this analysis are shown in Figure 17.

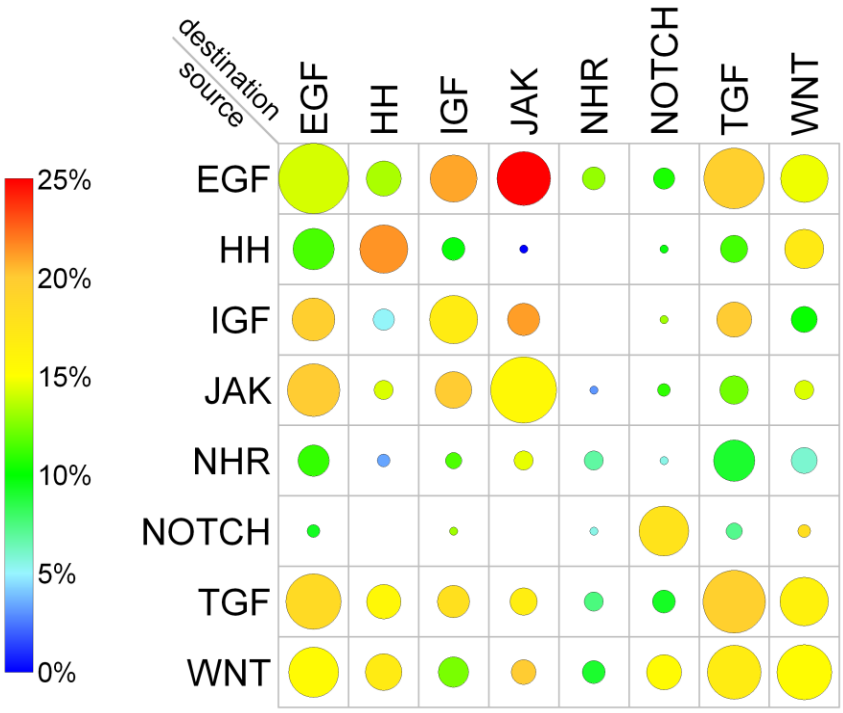

Figure 17. Differences in the frequency of altered cross-talks between $BRAF^{mut}$ and $BRAF^{wt}$ primary melanomas. The number of the cross-talks was visualized by varying circle size. The lack of circle means that there are no cross-talks between the pathways. The signal flow direction in the signaling interaction network is labeled as "source" or "destination" on the figure (i.e. a protein from the source pathway activates or inhibits a protein from the destination pathway). The calculated differences in the frequency of altered cross-talks between $BRAF^{mut}$ and $BRAF^{wt}$ tumor subtypes were displayed as heat map. For example red and orange color indicates on the figure that broad ranges of signaling interactions were more frequently altered (>20%) in $BRAF^{mut}$ melanoma compared to the $BRAF^{wt}$ tumor type within the HH and between the EGF-JAK, IGF-JAK and EGF-IGF pathways.

Cross-talk between the EGF (i.e EGF/MAPK pathway) and JAK networks was observed to be extensively altered in the $BRAF^{mut}$ tumors compared to the $BRAF^{wt}$ lesions. Additionally, interactions within the EGF-JAK, JAK-IGF and EGF-IGF pathways are more frequently altered (>20%). This analysis further supported the potentially important role of the HH pathway in $BRAF^{mut}$ primary melanoma.

CCND1 amplification in melanoma samples detected by Q-PCR

Based on the CGH data we selected the 11q13 region as a frequent alteration to define gene copy alterations in details. A total of 68 primary and 6 metastatic lesions were tested to identify CCND1 amplification by Q-PCR relative to the two reference genes (GNS and

UBE2E1). Using this technique CCDN1 amplification was found in 22 primary melanomas (32.4%) and in only one metastasis. The CCND1 gene amplification pattern was further compared in the primary and its metastatic tumor in four cases: the CCND1 gene was amplified in all the primary lesions (case numbers 5, 22, 8 and 13) but we could detect CCND1 amplification only in 1 metastasis (data not shown) (Table 9).

Evaluation of *TAOS1, FGF3, FGF4, FGF19* and *EMS1* gene copy numbers by Q-PCR

Samples with CCND1 amplification (22 primary melanomas) were further characterized for the TAOS1, FGF3, FGF4, FGF19 and EMS1 gene copy number alterations by Q-PCR. Among these 22 samples, 18.2% (4/22) showed amplification for all of these additional five genes (Table 9). In 45.5% of tumors (10/22) CCND1 was co-amplified with TAOS1; 36.4% (8/22) of CCND1 amplified tumors also displayed amplification of FGF3. Co-amplification of CCND1 and EMS1 was observed in 7 lesions (31.8%). The nine primary melanoma samples which exhibited higher CCND1 gene copy numbers (range 4.2-13.4) tended to display TAOS1 (7/9), FGF3 (6/9), FGF19 (6/9), FGF4 (6/9) and EMS1 (5/9) amplifications as well (see details in Table 9).

TABLE 9. Co-amplification of *TAOS1*, *FGF3*, *FGF19*, *FGF4* and *EMS1* with *CCND1* detected by Q-PCR and *BRAF* V600, *NRAS* Q61 mutations in primary melanomas.

	Relative gene copy number ± SE [1]							
Cases	***CCND1***	***TAOS1***	***FGF3***	***FGF19***	***FGF4***	***EMS1***	***BRAF*+ V600**	***NRAS* + Q61**
1	**13.4 ± 0. 60**	**10.0 ± 0. 71**	**5.00 ± 0. 61**	**7.4 ± 0. 65**	**7.9 ± 0. 62**	**5.8 ± 0. 48**	V600E	WT
2	**5.4 ± 0. 31**	**3.7 ± 0. 31**	**4.5 ± 0. 22**	**5.1 ± 0. 32**	**4.1 ± 0. 25**	**4.4 ± 0. 34**	WT	Q61R
3	**4.9 ± 0. 31**	**3.6 ± 0. 23**	**3.7 ± 0. 26**	**3.9 ± 0. 26**	**3.3 ± 0. 31**	**4.6 ± 0. 29**	V600E	WT
4	**4.4 ± 0. 34**	**4.4 ± 0. 27**	**3.3 ± 0. 38**	**7.4 ± 0. 65**	**3.7 ± 0. 26**	**5.2 ± 0. 32**	WT	WT
5	**11.7 ± 0. 34**	**7.0 ± 0. 44**	**3.8 ± 0. 23**	**4.9 ± 0. 36**	**4.0 ± 0. 44**	No Amp	WT	WT
6	**5.2 ± 0. 72**	**5.0 ± 0. 71**	**4.5 ± 0. 28**	**4.6 ± 0. 19**	**4.2 ± 0. 31**	No Amp	WT	WT
7	**3.2 ± 0. 10**	**3.0 ± 0. 22**	**3.3 ± 0. 13**	**3.8 ± 0. 22**	No Amp	**3.8 ± 0. 13**	WT	WT
8	**3.7 ± 0. 19**	**2.8 ± 0. 16**	**3.3 ± 0. 26**	No Amp	No Amp	No Amp	V600E	WT
9	**4.2 ± 0. 28**	**2.8 ± 0. 12**	No Amp	No Amp	No Amp	**3.8 ± 0. 13**	V600E	WT
10	**3.5 ± 0. 48**	**3.2 ± 0. 15**	No Amp	No Amp	No Amp	**3.0 ± 0. 06**	WT	WT
11	**9.6 ± 0. 74**	No Amp	No Amp	No Amp	No Amp	No Amp	WT	WT
12	**4.6 ± 0. 10**	No Amp	No Amp	No Amp	No Amp	No Amp	WT	WT
13	**3.8 ± 0. 24**	No Amp	No Amp	No Amp	No Amp	No Amp	WT	Q61K
14	**3.5 ± 0. 15**	No Amp	No Amp	No Amp	No Amp	No Amp	WT	Q61K
15	**3.4 ± 0. 22**	No Amp	No Amp	No Amp	No Amp	No Amp	WT	WT
16	**3.1 ± 0. 30**	No Amp	No Amp	No Amp	No Amp	No Amp	WT	Q61K
17	**3.1 ± 0. 12**	No Amp	No Amp	No Amp	No Amp	No Amp	WT	Q61K
18	**3.1 ± 0. 14**	No Amp	No Amp	No Amp	No Amp	No Amp	WT	Q61K
19	**3.0 ± 0. 19**	No Amp	No Amp	No Amp	No Amp	No Amp	V600E	WT
20	**3.0 ± 0. 16**	No Amp	No Amp	No Amp	No Amp	No Amp	V600R	WT
21	**2.9 ± 0. 09**	No Amp	No Amp	No Amp	No Amp	No Amp	WT	WT
22	**2.9 ± 0. 12**	No Amp	No Amp	No Amp	No Amp	No Amp	WT	Q61K

[1] Standard error
No Amp: amplification was not detected
WT: wild type *BRAF* or *NRAS* genotype

Correlation of gene alterations with clinicopathological parameters

In this analysis correlations were not find between CCND1 gene amplification status and any of the patients' clinicopathological parameters.

Tumors with CCND1 and TAOS1 co-amplification were classified with higher Clark's level (IV-V). Ulcerated tumors had a statistically significant association with CCND1 and TAOS1 co-amplification (p=0.017) (Table 10). In addition, co-amplification of CCND1 with TAOS1 (p<0.001), FGF3 (p=0.001), FGF19 (p<0.001), FGF4 (p=0.002) and EMS1 (p=0.004) genes, respectively, were more frequently found in thick (≥9 mm Breslow thickness) melanomas. Younger age at diagnosis was significantly associated with co-amplification of these five oncogenes (CCND1, TAOS1, FGF3, FGF19 and FGF4) (p=0.026, Mann-Whitney test) (data not shown).

NRAS codon 61 mutations were significantly more frequent in tumors originating from chronically sun-exposed sites (p= 0.005) (Table 10). Other clinical parameters did not show significant association with the prevalence of BRAF or NRAS mutations. However, an increased CCND1 gene copy number in conjunction with either BRAF or NRAS activation mutations was observed significantly more frequently in primary tumors with ulcerated surfaces (p=0.028) (data not shown).

Table 10. Associations of *CCND1* amplification, *CCND1/TAOS1* co-amplification, *BRAF* and *NRAS* mutation with clinicopathological parameters of patients.

	***CCND1*[1] n/total (%)**	**p**	***CCND1/TAOS1*[2] n/total (%)**	**p**	***BRAF*+[3] n/total (%)**	**p**	***NRAS*+[4] n/total (%)**	**p**
All tumor	22/68 (32)	-	10/68 (15)	-	25/68 (37)	-	13/68 (19)	-
Tumor Type[5]								
NM	10/26 (39)	0.433	4/26 (15)	1.000	9/26 (35)	0.802	7/26 (27)	0.220
SSM	12/42 (29)		6/42 (14)		16/42 (38)		6/42 (14)	
Gender								
Male	13/33 (39)	0.302	5/33 (15)	1.000	13/33 (39)	0.802	6/33 (18)	1.000
Female	9/35 (26)		5/35 (14)		12/35 (34)		7/35 (20)	
Age								
20-50	6/18 (33)	1.000	4/18 (22)	0.437	5/18 (28)	0.407	1/18 (6)	0.160
>50	16/50 (32)		6/50 (12)		20/50 (40)		12/50 (24)	
Breslow Thickness[6] (mm)								
<2.00	8/27 (30)		3/27 (11)		7/27 (26)		5/27 (19)	
2.01-4.00	3/13 (23)	0.430[7]	0/13 (0)	0.079[7]	7/13 (54)	0.801[7]	3/13 (23)	1.000[7]
>4.00	11/28 (39)		7/28 (25)		11/28 (39)		5/28 (18)	
Clark's level								
I, II, III	8/31 (26)	0.313	2/31 (7)	0.097	11/31 (36)	1.000	4/31 (13)	0.354
IV, V	14/37 (38)		8/37 (22)		14/37 (38)		9/37 (24)	
Ulceration								
Absent	7/31 (23)	0.129	1/31 (3)	0.017	9/31 (29)	0.313	5/31 (16)	0.758
Present	15/37 (41)		9/37 (24)		16/37 (43)		8/37 (22)	
Anatomic site								
Intermittently sun exposed site	17/53 (32)	1.000	7/53 (13)	0.680	21/53 (40)	0.545	6/53 (11)	0.005
Chronically sun exposed sites	5/15 (33)		3/15 (20)		4/15 (27)		7/15 (47)	
Metastasis formation[8]								
Nonmetastatic	7/25 (28)	0.406	2/25 (8)	0.273	8/25 (32)	1.000	4/25 (16)	0.350
Metastatic	13/32 (41)		7/32 (22)		11/32 (34)		9/32 (28)	

[1] Number of tumors with *CCND1* amplification
[2] Number of tumors with *CCND1/TAOS1* co-amplification
[3] Number of tumors with *BRAF* codon 600 mutation
[4] Number of tumors with *NRAS* codon 61 mutation
[5] NM, Nodular Melanoma; SSM, Superficial Spreading Melanoma
[6] Thickness categories based on the current melanoma staging system
[7] <4.00 mm versus >4.00mm
[8] Only patients with at least 3 years of follow up were included

Discussion

Melanoma consists of a heterogeneous group of tumors that differ in their types and range of genetic alterations. In order to identify novel therapeutic targets, and to develop successful therapies, it is essential to understand the molecular basis of cutaneous melanoma initiation and progression. It is accepted that high-resolution array CGH is able to detect small amplifications and deletions that potentially harbor specific oncogenes and tumor suppressor genes. In this study, through DNA copy-number profiling with array CGH analysis the aim was to discern differentially altered chromosomal segments and genes between BRAF- and NRAS-mutated melanoma subgroups.

Somatic mutations of BRAF and NRAS oncogenes are thought to be among the first steps in melanoma initiation. In our study the BRAFV600E was the most frequent mutation (26%) in the examined primary melanoma samples, which is in concordance with other studies [178, 179]. In addition, two other BRAF mutations were detected that were distinct from the V600E mutation. In each case, subsequent sequencing revealed the presence of V600K or V600R tandem mutations with a rate of 7% and 3%, respectively. The two most frequently observed NRAS mutations in the primary melanoma samples were Q61K and Q61R, with a rate of 10% and 7%, respectively, and these were associated exclusively with tumors derived from chronically sun exposed sites, a finding which agrees with past studies [109, 180]. After evaluating the mutational status of four primary-and-metastasis tumor pairs it was found that three metastatic lesions harbored the same mutations as the primary tumor from which they originated, which supports the idea that these mutations are preserved throughout melanoma progression [181].

Distinct genetic alterations were revealed between melanoma subgroups based on mutations of the BRAF and NRAS genes [10, 11, 95, 104]. Nevertheless, it is important to emphasize that only two of these articles provided data from primary melanomas. In concordance with these earlier reports a higher frequency of segmental chromosome 7 gain and chromosome 10 loss were found, which always included BRAF on 7q34 and PTEN on 10q23.3, that were found to be less frequent in WT tumors or in NRAS mutated lesions. Unsupervised hierarchical clustering of common tumor-associated regions at the 10q chromosomal arm also revealed that their deletion patterns are linked to high-grade tumors and to the presence of $BRAF^{mut}$. This observation is consistent with a previous model which suggests a cooperative effect

between the PTEN (10q23.31) and BRAF (7q34) cancer genes in melanoma [127]. It has been implied in several recent studies that the inactivation of the PTEN tumor suppressor gene is a key genetic event in melanoma [125]. On the other hand, whereas extended deletions on chromosome 10 suggest a novel theory wherein a broad range of chromosome 10 losses in conjunction with BRAF activation and PTEN inactivation may be involved in polygenic melanoma tumorigenesis. The 7q36.3 region harboring the PTPRN2 gene was found to be one of the most frequent high-level amplifications (14% of primary melanomas) and was also linked to the presence of $BRAF^{mut}$. The product of this gene acts as a signaling molecule involved in cell growth, differentiation, mitosis and oncogenic transformation. In a recent study, the downregulation of a set of genes, including the PTPRN2, was able to suppress metastasis of breast cancer cells to different organ sites [182].

Furthermore, loss of 11q23.3-11q25, which carries the well-established tumor suppressor gene named OPCML, was mainly associated with $NRAS^{mut}$ primary melanoma. This observation indicates another possible link between loss in this region and the consecutive activation of NRAS protein [183]. Moreover the loss of one allele at 17p13.3 was also observed frequently in $NRAS^{mut}$ melanomas. This tumor suppressor locus on 17p has already been observed in brain, breast, lung, and ovarian tumors [184-187], they indentified two candidate tumor suppressor genes HIC1 and OVCA1 at this locus [186, 188, 189]. It was also suggested that the reduction to hemizygosity of 17p13.3 resulted in cell cycle deregulation and promote tumorigenesis in ovarian cancer cells [189].

Additionally, the group of tumors with BRAF or NRAS mutations also frequently showed deletions and amplification in the 9p including the loci of CDKN2A (9p21.3) and in the 6p22.3 chromosomal region, respectively. The E2F3 candidate gene at the 6p22.3 region was already found to be over-expressed in several bladder tumor cell lines with 6p22.3 amplification and knock-down of E2F3 resulted in reduced proliferation of cells [190] (see the summarized data in Figure 18).

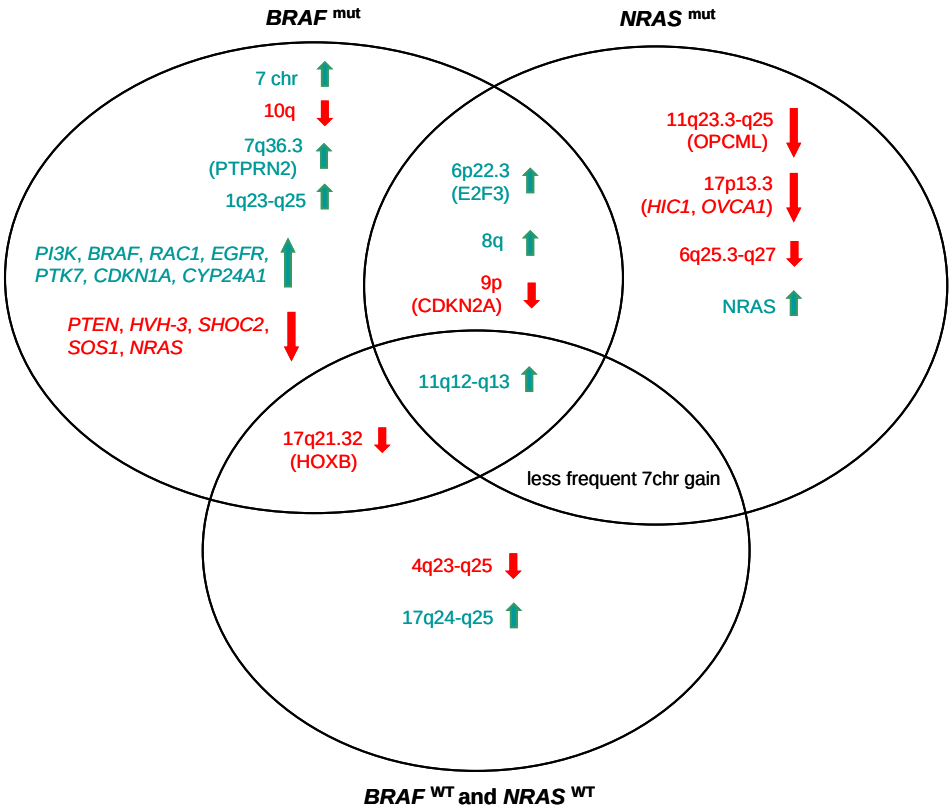

Figure 18. The summary of the major common and distinct copy number alterations among the three mutation subgroups. The up and green arrow indicates gain of a given chromosomal region or gene, and the down red arrow indicates their loss.

It is well known that genetic events at different genomic regions act concordantly in tumor development. Therefore, a correlation analysis was performed between BAC clones frequently changed in the investigated tumor subgroups in order to identify regions of chromosomal loss and gain that commonly coexist in BRAF^{mut} or WT primary melanomas. It has to be mentioned that this analysis was done on a relatively small set of tumors so it only begins to address the possible combinations of cooperating regions. The heat maps on Figure 14 show trends of correlation between chromosomal regions in the two different melanoma subgroups.

Activation of the EGF/MAPK pathway via genetic alterations is thought to be a main causative factor during melanoma development, and their inhibition sensitizes melanoma cells to certain anticancer agents [135]. Our aim was to explore a relevant subset of gene copy number alterations that have important impacts on dysregulation of the EGF/MAPK pathway along with the BRAF mutation. A more complete understanding of the genetic alterations that co-occur with mutations of BRAF could help to identify therapies that may act synergistically with BRAF kinase inhibitors. The selection of relevant genes for sample classification is one

of the challenges in most microarray studies where researchers try to identify the smallest possible set of chromosomal loci or genes that can still achieve good predictive performance. Random forest analysis is getting more and more widely used in the field of the evaluation of microarray experiments because it has several characteristics that make it ideal to investigate these data sets, such as a) when the number of variables are much larger than the number of observations and b) when datasets contain a large number of noisy variables [191-193]. With this method, a particular deletion pattern involving three well-known cancer genes, such as PTEN, HVH-3 and JNK1 were identified and found to be associated with BRAF mutation. PTEN is a well-known tumor suppressor gene, but little data has been published on the role of HVH-3 and JNK1 in melanoma tumorigenesis. According to the literature, the expression of HVH-3 resulted in both the specific inactivation and the nuclear translocation of ERK2 [194] and it has been proven that silencing the ERK2 mRNA inhibits tumor growth in vivo [195]. There is also further evidence for the role of JNK1 gene in tumorigenesis: failure of the function of JNK1 could facilitate tumor formation and $JNK1^{-/-}$ mice developed spontaneous intestinal tumors [196, 197]. We identified, moreover, a group of other genes to be associated with BRAF mutation, including SHC1, PEA15, ELK4, EGFR and PI3K that have evidence of oncogenic activity or may be potential anti-cancer treatment targets [198, 199]. We also observed that their concomitant amplifications were highly predictive for BRAF mutation.

Moreover, exploring the frequency of the significantly more frequently altered cross-talks among $BRAF^{mut}$ and $BRAF^{wt}$ melanomas revealed the significant importance of cross-talks between the MAPK-JAK, MAPK-IGF and JAK-IGF pathways and in the HH pathway in BRAF mutated melanoma progression.

During the array CGH analysis of 47 primary melanomas, we observed a common large regional gains in 11q13 chromosome region, which has been also reported by previous studies with conventional cytogenetic and comparative genomic hybridization methods [71, 74, 200]. In order to investigate detailed gene copy number alterations in the 11q13 amplicon core in primary and metastatic melanomas a Q-PCR was elaborated. Since it was found that CCND1 is co-amplified with other genes located within the 11q13 region in several malignancies, and it is likely these co-amplifications play a pathogenic role in those cancers [82, 83, 92].

In order to define the co-amplification pattern of genes in the 11q13 amplicon, a Q-PCR assay was designed for the CCND1, TAOS1, FGF3, FGF19, FGF4 and EMS1 gene copy number determination. We found that 32% of the primary melanomas exhibited amplification of the CCND1 gene. These data support the importance of the CCND1 amplification in promoting cell proliferation in subgroups of primary melanomas. However, the CCND1 amplification

frequencies between primary and metastatic sites can indicate that this genetic aberration probably not obligatory for the metastatic process because it is not selected during the metastatic process. Although, further detailed examinations are needed to verify this hypothesis because of the relatively low number of primer-meta tumor sample pairs analysed. The co-amplification of CCND1 with TAOS1 was another frequent event in this region and had a significant association with the presence of ulceration (p=0.017), a clinical feature that can predict poor prognosis. TAOS1 has been described as a possibly important gene that might drive the 11q13 amplification in oral squamous cell carcinoma (OSCC) [83] and it may be a novel marker gene for advanced types of esophageal squamous cell carcinoma [79]. An association between TAOS1 gene amplification and larger tumor size, the presence of lymph node metastasis, poor histological differentiation and advanced clinical stage in OSCC has been found [80]. RNA interference method predicts that TAOS1 would participate in cell cycle control and regulate cell proliferation, similarly to CCND1 [80]. In this work it was also shown that co-amplifications of each of these genes (TAOS1, FGF3, FGF19, FGF4 and EMS1) with CCND1 are characteristic for thick primary melanomas, and co-amplification of these are present in patients of younger age. It is also known, that FGF3 and FGF4 are secreted glycoproteins that are generally readily sequestered to the extracellular matrix, as well as the cell surface, by heparan sulphate proteoglycans and the FGFR2 (fibroblast growth factor receptor) is regulated on the basis of the balance of FGF3 and FGF4. FGFR2 transduces FGF signals to MAPK, PI3K signaling cascades. Aberrant FGF signalling can promote tumour development by directly driving cancer cell proliferation and survival [201]. Based on the observed data we assume that co-amplification of these candidate genes can contribute to a more aggressive phenotype than CCND1 amplification alone. However, it is possible that the co-amplifications are merely a result of genetic instability that increases as the tumor progresses and that these genes do not contribute directly to the phenotypic alterations [202].

In this work another aim was to evaluate the relationship between increased CCND1 gene dosage and the frequency of BRAF and NRAS mutations and found that 34% of the primary melanomas harboring one of these activating mutations also had CCND1 alterations. Among these tumors, melanomas with ulcerated surfaces were significantly more frequently present (p=0.028), indicating the clinical relevance of this finding. This link is supported by a recent study in which CCND1 was found to be amplified in 17% of BRAF V600E-mutated human metastatic melanoma samples and its overexpression, resulting from genomic amplification, increased BRAF inhibitor resistance of BRAF V600E-mutated melanomas [203].

In conclusion, molecular alterations were distinguished between different melanoma subtypes. These marked differences in the genetic pattern of the BRAF or NRAS mutated and WT melanoma subgroups confirm the involvement of distinct genetic pathways in melanoma tumorigenesis that are driven either through BRAF or NRAS mutations. Here was also found that neither the increased CCND1 gene dosage nor the BRAF or the NRAS mutations alone contributed to more aggressive phenotype. However, we assume that co-amplification of other candidate oncogenes in the 11q13 region or carrying a CCND1 alteration along with either the activating BRAF or NRAS mutation may be more important for prognosis in subgroups of aggressive melanomas than the presence of these alterations alone. Investigating the non-random correlation of gene alterations could distinguish oncogenic modules that contain driver genes involved in the progression of melanoma.

Conclusions

This thesis is aimed to better characterize the possible association of BRAF and NRAS mutations with marked genetic alterations in primary melanoma:

The main conclusions are:

- Melanomas with the presence of BRAF mutation exhibited more frequent losses on 10q23-q26 and gains on chromosome 7 and 1q23-q25. Loss on the 11q23-q25 sequence was found mainly in conjunction with NRAS mutation. Hierarchical cluster analysis revealed that the presence of BRAF mutation is associated with deletion pattern on 10q chromosome and is frequently observed in lesions with advanced clinical stages.

- Correlation analysis revealed chromosomal alterations that coexist more often in the different subgroups of primary melanomas ($BRAF^{mut}$, WT).

- Investigating the specific dynamic activities among eight different signaling highlighted the frequent alterations of genes involved in the protein-protein interactions between the MAPK-JAK pathways in BRAF mutated primary melanomas.

- We also found a gene alteration signature in the MAPK pathway that was commonly related to the presence of the BRAF mutation in our melanoma cohorts.

- After developing an accurate Q-PCR method for determining the co-amplification pattern of six candidate genes that reside in the 11q13 amplicon core, we found that coamplification of these candidate genes or the CCND1 amplification along with either

BRAF or NRAS mutations indicating that they are more important for prognosis than the presence of these alterations alone.

Based on these results we were able to prove the existence of marked differences in the genetic pattern of the BRAF and NRAS mutated melanoma subgroups that might suggest that these mutations contribute to malignant melanoma in conjunction with distinct cooperating oncogenic events. These additional oncogenic events which are associated with BRAF or NRAS mutations can provide rational additional targets for a combination therapy with kinase inhibitors. However, more detailed investigations are desperately needed to find out that how these different mutational profiles and molecular subgroupings can be translated into novel strategies for the treatment of melanoma.

Summary

Human malignant melanoma is one of the most aggressive forms of skin cancer with an exceptionally bad prognosis. Melanoma often display constitutively activated MAPK pathway through BRAF or NRAS mutations. It is also known that these mutations are almost never simultaneously present and that they appear at early stages and preserved throughout tumor progression, although it is proved that these alterations alone are insufficient to cause tumor progression. Therefore the first aim of our study was to evaluate those distinct genetic alterations which can properly differentiate the three important molecular subtypes of primary melanomas with a) BRAF, b) NRAS mutation andc) WT (wild type for both loci). Mutation analysis in the BRAF and NRAS oncogene was performed by melting curve analysis using fluorescent probes. High-resolution array comparative genomic hybridization (array CGH) was used to assess genome-wide analysis of DNA copy number alterations. Based on our array CGH data primary melanomas with BRAF mutation exhibited more frequent losses on 10q23-q26 and gains on chromosome 7 and 1q23-q25 compared to melanomas with NRAS mutation. Loss on the 11q23-q25 sequence was found mainly in conjunction with NRAS mutation. Hierarchical cluster analysis revealed that the presence of BRAF mutation is associated with deletion pattern on 10q chromosome and is frequently observed in lesions with advanced clinical stages. Based on these results we proved the existence of marked differences in the genetic pattern of the BRAF and NRAS mutated melanoma subgroups that might suggest that these mutations contribute to malignant melanoma in conjunction with distinct cooperating oncogenic events. In general, it is an interesting phenomenon suggesting that these mutations provide probably the ‘guiding force’ for these tumors and it also suggests

that there are alternative genetic pathways to melanoma. These additional oncogenic events which are associated with BRAF or NRAS mutations can provide rational additional targets for a combination therapy with kinase inhibitors. In this study we also investigated the specific dynamic activities among different signaling pathways highlighted the frequent alterations of genes involved in the signaling interactions between the MAPK-JAK pathways in BRAF mutated melanomas. Using Random Forest analysis we also found a gene alteration signature in the MAPK pathway that was commonly related to the presence of the *BRAF* mutation in our melanoma cohorts. The second aim of this study was to develop an accurate Q-PCR method for determining the co-amplification pattern of six candidate genes that reside in the 11q13 amplicon core. We found that coamplification of these candidate genes or the CCND1 amplification along with either BRAF or NRAS mutations might be more important for prognosis than the presence of these alterations alone.

Összefoglalás (in hungarian)

A malignus melanoma az egyik legagresszívabb bőrdaganat, melyek jelentős része rendkívül rossz prognózissal jellemezhető. A melanomák többségében a MAP-kináz útvonal konstitutívan aktiválódik, melyet az NRAS vagy BRAF onkogének mutációja okoz a melanomák tumorigenezisének korai fázisában. Ezen mutációkról már leírták, hogy a daganat progresszió során végig fennmaradnak. A mutációk jelenlétének és prognosztikai jelentőségének eddigi vizsgálatai viszont kimutatták, hogy ezeknek a mutációknak egyedüli jelenléte viszont még nem elegendő a daganatok kialakulásához. Vizsgálataink során kiemelt figyelmet szenteltünk a *BRAF* és *NRAS* mutációt hordozó primer melanomák jellegzetes molekuláris eltéréseinek megismerése. A teljes genom eltéréseinek analízisére array-CGH-et alkalmaztunk. A mutációk jelenlétét floureszcensen jelölt oligonukleotid próbák segítségével, olvadáspont analízissel vizsgáltuk. A BRAF-mutációt hordozó daganatokban a leggyakoribb eltérések az 1-es kromoszóma hosszú karjának, illetve a teljes 7-es kromoszómának a DNS-többlete és a 10-es kromoszóma hosszú karjának DNS-hiánya voltak. Az NRAS-mutációt hordozó daganatokra a 11q22.3-11q25 régióban gyakran előforduló deléció volt jellemező. Hierarchikus klaszter analízisünk szerint a 10-es kromoszóma hosszú karjának deléciója szignifikánsan gyakrabban fordul elő BRAF mutációt hordozó és előrehaladott stádiumban lévő primer daganatokban. Eredményeink alapján feltételezhetjük, hogy annak ellenére, hogy az NRAS és a BRAF onkogének aktivációs mutációi ugyanazon szignáltranszdukciós útvonalat aktiválják, a primer melanomák tumorigenezise során eltérő genetikai alterációkkal kooperálnak. Ez a melanoma progresszió során tapasztalt jelenség rendkívül figyelemre

méltó, hiszen arra utalhat, hogy a BRAF és NRAS mutációk egyfajta vezérlő erőként funkcionálnak az alternatív genetikai útvonalakat feltételező melanomagenezis során. Eredményeink elemzése során a különböző szignál transzdukciós útvonalak részletesebb vizsgálatával felderítettük, hogy a BRAF mutációt hordozó daganatokban leggyakrabban a MAPK-JAK szignalizációs útvonalak közötti interakcióban résztvevő fehérjék génjei sérülnek majd Random Forest analízis segítségével azonosítottunk további BRAF mutációval összefüggésbe hozható gyakori gén kópiaszám eltéréseket a MAPK útvonalból. Valamint részletesen tanulmányoztuk a 11q13 amplifikációs régió géneltéréseit, melyet korábbi CGH vizsgálataink során a melanoma egyik leggyakoribb genetikai eltéréseként azonosítottunk. Eredményeink arra utalnak, hogy a 11q13 régióban lokalizálódó onkogének ko-amplifikációja, a BRAF vagy NRAS mutáció együttes előfordulása a CCND1 emelkedett géndózisával társulva gyakrabban jellemző rossz prognózisú daganatokra, mint ezen genetikai eltérések jelenléte külön-külön.

List of original publications

This thesis is based on the following original publications:

Lázár V., Ecsedi S., Szöllosi AG., Tóth R., Vízkeleti L., Rákosy Z., Bégány A., Adány R., Balázs M. Characterization of candidate gene copy number alterations in the 11q13 region along with BRAF and NRAS mutations in human melanoma. Mod Pathol., 2009 Oct;22(10):1367-78.
IF: 4.406

Lázár V., Ecsedi S., Vízkeleti L., Rákosy Z., Boross G., Szappanos B., Bégány A., Emri G., Ádány R., Balázs M. Marked genetic differences between BRAF and NRAS mutated primary melanomas as revealed by array comparative genomic hybridization. Melanoma Res. 2012 Jun;22(3):202-14.
IF: 2.187 (2011)

Other original publications:

Barok, M., Balazs, M., **Lazar, V.,** Rakosy, Z., Toth, E., Treszl, A., Vereb, G., Colbern, G.T., Park, J.W., Szollosi, J. Characterization of a novel, trastuzumab resistant human breast cancer cell line. Frontiers in bioscience 2010. 2:627-640.
IF: - (2010)

Vízkeleti L., Ecsedi S., Rákosy Z., Orosz A., **Lázár V.,** Emri G., Koroknai V., Kiss T., Ádány R., Balázs M. The role of CCND1 alterations during the progression of cutaneous malignant melanoma.Tumour Biol., 2012 Sept 23., [Epub ahead of print]
IF: 2.143 (2011)

Rakosy Z, Ecsedi S, Toth R, Vizkeleti L, Herandez-Vargas H, **Lazar V,** Emri G, Szatmari I, Herceg Z, Adany R, Balazs M. Integrative genomics identifies gene signature associated with melanoma ulceration. PLoS One. 2013;8(1):e54958. Epub 2013 Jan 30.
IF: 4.092 (2011)

Register Number: DEENKÉTK/123/2013.
Item Number:
Subject: Ph.D. List of Publications

Candidate: Viktória Lázár

Neptun ID: QYNYLP

Doctoral School: Doctoral School of Health Sciences

List of publications related to the dissertation

1. **Lázár, V.**, Ecsedi, S., Vízkeleti, L., Rákosy, Z., Boross, G., Szappanos, B., Bégány, Á., Emri, G., Ádány, R., Balázs, M.: Marked genetic differences between BRAF and NRAS mutated primary melanomas as revealed by array comparative genomic hybridization.
Melanoma Res. 22 (3), 202-214, 2012.
DOI: http://dx.doi.org/10.1097/CMR.0b013e328352dbc8
IF:2.187 (2011)

2. **Lázár, V.**, Ecsedi, S., Szöllősi, A., Tóth, R., Vízkeleti, L., Rákosy, Z., Bégány, Á., Ádány, R., Balázs, M.: Characterization of candidate gene copy number alterations in the 11q13 region along with BRAF and NRAS mutations in human melanoma.
Mod. Pathol. 22 (10), 1367-1378, 2009.
DOI: http://dx.doi.org/10.1038/modpathol.2009.109
IF:4.406

List of other publications

3. Rákosy, Z., Ecsedi, S., Tóth, R., Vízkeleti, L., Herandez-Vargas, H., **Lázár, V.**, Emri, G., Szatmári, I., Herceg, Z., Ádány, R., Balázs, M.: Integrative genomics identifies gene signature associated with melanoma ulceration.
PLoS One. 8 (1), e54958, 2013.
DOI: http://dx.doi.org/10.1371/journal.pone.0054958
IF:4.092 (2011)

4. Vízkeleti, L., Ecsedi, S., Rákosy, Z., Orosz, A., **Lázár, V.**, Emri, G., Koroknai, V., Kiss, T., Ádány, R., Balázs, M.: The role of CCND1 alterations during the progression of cutaneous malignant melanoma.
Tumor Biol. 33 (6), 2189-2199, 2012.
DOI: http://dx.doi.org/10.1007/s13277-012-0480-6
IF:2.143 (2011)

5. Barok, M., Balázs, M., **Lázár, V.**, Rákosy, Z., Tóth, E., Treszl, A., Vereb, G., Colbern, G.T., Park, J.W., Szöllősi, J.: Characterization of a novel, trastuzumab resistant human breast cancer cell line.
Front. Biosci. (Elite Ed). 1 (2), 627-640, 2010.

6. Balázs, M., Barok, M., **Lázár, V.**, Rákosy, Z., Toth, E., Park, J., Szöllősi, J.: Genomic and gene expression characterization of a novel trastuzumab-resistant breast cancer cell line.
Eur. J. Cancer. Suppl. 6 (9), 119, 2008.

Total IF: 12.828

Total IF (publications related to the dissertation): 6.593

The Candidate's publication data submitted to the Publication Database of the University of Debrecen have been validated by Kenezy Life Sciences Library on the basis of Web of Science, Scopus and Journal Citation Report (Impact Factor) databases.

28 March, 2013

References

1. Jemal, A., Siegel, R., Xu, J. & Ward, E. Cancer statistics, 2010. *CA Cancer J Clin* **60**, 277-300 (2010).

2. Yoshida, H. et al. Review: melanocyte migration and survival controlled by SCF/c-kit expression. *J Investig Dermatol Symp Proc* **6**, 1-5 (2001).

3. Slominski, A., Tobin, D.J., Shibahara, S. & Wortsman, J. Melanin pigmentation in mammalian skin and its hormonal regulation. *Physiol Rev* **84**, 1155-228 (2004).

4. Dessinioti, C., Stratigos, A.J., Rigopoulos, D. & Katsambas, A.D. A review of genetic disorders of hypopigmentation: lessons learned from the biology of melanocytes. *Exp Dermatol* **18**, 741-9 (2009).

5. Lin, J.Y. & Fisher, D.E. Melanocyte biology and skin pigmentation. *Nature* **445**, 843-50 (2007).

6. Meric, J.B., Rixe, O. & Khayat, D. Metastatic malignant melanoma. *Drugs Today (Barc)* **39 Suppl C**, 17-38 (2003).

7. Kudchadkar, R. Novel targeted therapies for the treatment of metastatic melanoma. *Ochsner J* **10**, 117-24 (2010).

8. Haass, N.K., Smalley, K.S. & Herlyn, M. The role of altered cell-cell communication in melanoma progression. *J Mol Histol* **35**, 309-18 (2004).

9. Welch, D.R. & Goldberg, S.F. Molecular mechanisms controlling human melanoma progression and metastasis. *Pathobiology* **65**, 311-30 (1997).

10. Greshock, J. et al. Distinct patterns of DNA copy number alterations associate with BRAF mutations in melanomas and melanoma-derived cell lines. *Genes Chromosomes Cancer* **48**, 419-28 (2009).

11. Curtin, J.A. et al. Distinct sets of genetic alterations in melanoma. *N Engl J Med* **353**, 2135-47 (2005).

12. Ribas, A. & Flaherty, K.T. BRAF targeted therapy changes the treatment paradigm in melanoma. *Nat Rev Clin Oncol* **8**, 426-33 (2011).

13. Lens, M. Current clinical overview of cutaneous melanoma. *Br J Nurs* **17**, 300-5 (2008).

14. Thompson, J.F., Scolyer, R.A. & Kefford, R.F. Cutaneous melanoma. *Lancet* **365**, 687-701 (2005).

15. Leiter, U. & Garbe, C. Epidemiology of melanoma and nonmelanoma skin cancer--the role of sunlight. *Adv Exp Med Biol* **624**, 89-103 (2008).

16. Kabigting, F.D. et al. Malignant melanoma in African-Americans. *Dermatol Online J* **15**, 3 (2009).

17. Balatoni, T., Liszkay, G., Miklos, Z. & Kasler, M. [Epidemiology of malignant melanoma (Clinical experience at the National Institute of Oncology in Hungary).]. *Orv Hetil* **152**, 1000-1006 (2011).

18. Vogelstein, B. & Kinzler, K.W. The multistep nature of cancer. *Trends Genet* **9**, 138-41 (1993).

19. Clark, W.H., Jr. et al. A study of tumor progression: the precursor lesions of superficial spreading and nodular melanoma. *Hum Pathol* **15**, 1147-65 (1984).

20. Meier, F. et al. Molecular events in melanoma development and progression. *Front Biosci* **3**, D1005-10 (1998).

21. NIH Consensus conference. Diagnosis and treatment of early melanoma. *Jama* **268**, 1314-9 (1992).

22. Uong, A. & Zon, L.I. Melanocytes in development and cancer. *J Cell Physiol* **222**, 38-41 (2010).

23. Goldman, B.D. Melanoma and tumor thickness. *Arch Dermatol* **136**, 122-3 (2000).

24. Markovic, S.N. et al. Malignant melanoma in the 21st century, part 1: epidemiology, risk factors, screening, prevention, and diagnosis. *Mayo Clin Proc* **82**, 364-80 (2007).

25. Cohen, L.M. Lentigo maligna and lentigo maligna melanoma. *J Am Acad Dermatol* **36**, 913 (1997).

26. Char, D.H. Ocular melanoma. *Surg Clin North Am* **83**, 253-74, vii (2003).

27. Livestro, D.P. et al. Biology of desmoplastic melanoma: a case-control comparison with other melanomas. *J Clin Oncol* **23**, 6739-46 (2005).

28. Rousseau, D.L., Jr. & Gershenwald, J.E. The new staging system for cutaneous melanoma in the era of lymphatic mapping. *Semin Oncol* **31**, 415-25 (2004).

29. Gershenwald, J.E., Soong, S.J. & Balch, C.M. 2010 TNM staging system for cutaneous melanoma...and beyond. *Ann Surg Oncol* **17**, 1475-7 (2010).

30. Olah, J. & Dobozy, A. [The new TNM classification of malignant melanoma]. *Magy Onkol* **47**, 59-61 (2003).

31. Chin, L., Merlino, G. & DePinho, R.A. Malignant melanoma: modern black plague and genetic black box. *Genes Dev* **12**, 3467-81 (1998).

32. Breslow, A. Thickness, cross-sectional areas and depth of invasion in the prognosis of cutaneous melanoma. *Ann Surg* **172**, 902-8 (1970).

33. Clark, W.H., Jr., From, L., Bernardino, E.A. & Mihm, M.C. The histogenesis and biologic behavior of primary human malignant melanomas of the skin. *Cancer Res* **29**, 705-27 (1969).

34. Hemo, Y., Gutman, M. & Klausner, J.M. Anatomic site of primary melanoma is associated with depth of invasion. *Arch Surg* **134**, 148-50 (1999).

35. Martorell-Calatayud, A., Requena, C., Botella-Estrada, R. & Sangueza, O.P. [Advances in molecular biology and their application in the diagnosis and treatment of melanoma]. *Actas Dermosifiliogr* **100 Suppl 1**, 52-65 (2009).

36. Thorn, M., Ponten, F., Bergstrom, R., Sparen, P. & Adami, H.O. Clinical and histopathologic predictors of survival in patients with malignant melanoma: a population-based study in Sweden. *J Natl Cancer Inst* **86**, 761-9 (1994).

37. Balch, C.M. et al. Final version of the American Joint Committee on Cancer staging system for cutaneous melanoma. *J Clin Oncol* **19**, 3635-48 (2001).

38. Bandarchi, B., Ma, L., Navab, R., Seth, A. & Rasty, G. From melanocyte to metastatic malignant melanoma. *Dermatol Res Pract* **2010** (2010).

39. MacKie, R.M., Hauschild, A. & Eggermont, A.M. Epidemiology of invasive cutaneous melanoma. *Ann Oncol* **20 Suppl 6**, vi1-7 (2009).

40. Ikehata, H. & Ono, T. The mechanisms of UV mutagenesis. *J Radiat Res (Tokyo)* **52**, 115-25 (2011).

41. Ichihashi, M. et al. UV-induced skin damage. *Toxicology* **189**, 21-39 (2003).

42. Maverakis, E. et al. Light, including ultraviolet. *J Autoimmun* **34**, J247-57 (2011).

43. Elwood, J.M. & Jopson, J. Melanoma and sun exposure: an overview of published studies. *Int J Cancer* **73**, 198-203 (1997).

44. Bevona, C., Goggins, W., Quinn, T., Fullerton, J. & Tsao, H. Cutaneous melanomas associated with nevi. *Arch Dermatol* **139**, 1620-4; discussion 1624 (2003).

45. McMeniman, E., De'Ambrosis, K. & De'Ambrosis, B. Risk factors in a cohort of patients with multiple primary melanoma. *Australas J Dermatol* **51**, 254-7 (2010).

46. Ford, D. et al. Risk of cutaneous melanoma associated with a family history of the disease. The International Melanoma Analysis Group (IMAGE). *Int J Cancer* **62**, 377-81 (1995).

47. Kamb, A. et al. Analysis of the p16 gene (CDKN2) as a candidate for the chromosome 9p melanoma susceptibility locus. *Nat Genet* **8**, 23-6 (1994).

48. Hussussian, C.J. et al. Germline p16 mutations in familial melanoma. *Nat Genet* **8**, 15-21 (1994).

49. Zuo, L. et al. Germline mutations in the p16INK4a binding domain of CDK4 in familial melanoma. *Nat Genet* **12**, 97-9 (1996).

50. Serrano, M., Hannon, G.J. & Beach, D. A new regulatory motif in cell-cycle control causing specific inhibition of cyclin D/CDK4. *Nature* **366**, 704-7 (1993).

51. Sherr, C.J. & Weber, J.D. The ARF/p53 pathway. *Curr Opin Genet Dev* **10**, 94-9 (2000).

52. Bishop, D.T. et al. Geographical variation in the penetrance of CDKN2A mutations for melanoma. *J Natl Cancer Inst* **94**, 894-903 (2002).

53. Soufir, N. et al. Prevalence of p16 and CDK4 germline mutations in 48 melanoma-prone families in France. The French Familial Melanoma Study Group. *Hum Mol Genet* **7**, 209-16 (1998).

54. Tucker, M.A. & Goldstein, A.M. Melanoma etiology: where are we? *Oncogene* **22**, 3042-52 (2003).

55. Valverde, P., Healy, E., Jackson, I., Rees, J.L. & Thody, A.J. Variants of the melanocyte-stimulating hormone receptor gene are associated with red hair and fair skin in humans. *Nat Genet* **11**, 328-30 (1995).

56. Diefenbach, K., Mrozikiewicz, P.M., Brien, B., Landt, O. & Roots, I. Rapid genotyping of melanocortin-1 receptor with use of fluorescence-labeled oligonucleotides. *Clin Chem* **49**, 507-9 (2003).

57. Lin, J., Hocker, T.L., Singh, M. & Tsao, H. Genetics of melanoma predisposition. *Br J Dermatol* **159**, 286-91 (2008).

58. Box, N.F. et al. MC1R genotype modifies risk of melanoma in families segregating CDKN2A mutations. *Am J Hum Genet* **69**, 765-73 (2001).

59. Lang, J., Boxer, M. & MacKie, R. Absence of exon 15 BRAF germline mutations in familial melanoma. *Hum Mutat* **21**, 327-30 (2003).

60. Blokx, W.A., van Dijk, M.C. & Ruiter, D.J. Molecular cytogenetics of cutaneous melanocytic lesions - diagnostic, prognostic and therapeutic aspects. *Histopathology* **56**, 121-32 (2010).

61. Miller, A.J. & Mihm, M.C., Jr. Melanoma. *N Engl J Med* **355**, 51-65 (2006).

62. Van Raamsdonk, C.D. et al. Frequent somatic mutations of GNAQ in uveal melanoma and blue naevi. *Nature* **457**, 599-602 (2009).

63. Pollock, P.M. & Trent, J.M. The genetics of cutaneous melanoma. *Clin Lab Med* **20**, 667-90 (2000).

64. Brose, M.S. et al. BRAF and RAS mutations in human lung cancer and melanoma. *Cancer Res* **62**, 6997-7000 (2002).

65. Trent, J.M. et al. Relation of cytogenetic abnormalities and clinical outcome in metastatic melanoma. *N Engl J Med* **322**, 1508-11 (1990).

66. Liu, L. et al. Mutation of the CDKN2A 5' UTR creates an aberrant initiation codon and predisposes to melanoma. *Nat Genet* **21**, 128-32 (1999).

67. Kraehn, G.M. et al. Extra c-myc oncogene copies in high risk cutaneous malignant melanoma and melanoma metastases. *Br J Cancer* **84**, 72-9 (2001).

68. Anderson, G.R., Stoler, D.L. & Brenner, B.M. Cancer: the evolved consequence of a destabilized genome. *Bioessays* **23**, 1037-46 (2001).

69. Bastian, B.C., LeBoit, P.E., Hamm, H., Brocker, E.B. & Pinkel, D. Chromosomal gains and losses in primary cutaneous melanomas detected by comparative genomic hybridization. *Cancer Res* **58**, 2170-5 (1998).

70. Nelson, M.A. et al. Chromosome abnormalities in malignant melanoma: clinical significance of nonrandom chromosome abnormalities in 206 cases. *Cancer Genet Cytogenet* **122**, 101-9 (2000).

71. Bastian, B.C., Olshen, A.B., LeBoit, P.E. & Pinkel, D. Classifying melanocytic tumors based on DNA copy number changes. *Am J Pathol* **163**, 1765-70 (2003).

72. Hsu, C.P. et al. Clinical significance of tumor suppressor PTEN in colorectal carcinoma. *Eur J Surg Oncol* **37**, 140-7 (2010).

73. Slominski, A. et al. Malignant melanoma. *Arch Pathol Lab Med* **125**, 1295-306 (2001).

74. Balazs, M. et al. Chromosomal imbalances in primary and metastatic melanomas revealed by comparative genomic hybridization. *Cytometry* **46**, 222-32 (2001).

75. Yurakh, A.O. et al. Molecular and immunohistochemical analysis of the prognostic value of cell-cycle regulators in urothelial neoplasms of the bladder. *Eur Urol* **50**, 506-15; discussion 515 (2006).

76. Akervall, J. et al. Chromosomal translocations involving 11q13 contribute to cyclin D1 overexpression in squamous cell carcinoma of the head and neck. *Int J Oncol* **20**, 45-52 (2002).

77. Elsheikh, S. et al. CCND1 amplification and cyclin D1 expression in breast cancer and their relation with proteomic subgroups and patient outcome. *Breast Cancer Res Treat* **109**, 325-35 (2008).

78. Rodrigo, J.P., Garcia, L.A., Ramos, S., Lazo, P.S. & Suarez, C. EMS1 gene amplification correlates with poor prognosis in squamous cell carcinomas of the head and neck. *Clin Cancer Res* **6**, 3177-82 (2000).

79. Komatsu, Y. et al. TAOS1, a novel marker for advanced esophageal squamous cell carcinoma. *Anticancer Res* **26**, 2029-32 (2006).

80. Xia, J., Chen, Q., Li, B. & Zeng, X. Amplifications of TAOS1 and EMS1 genes in oral carcinogenesis: association with clinicopathological features. *Oral Oncol* **43**, 508-14 (2007).

81. Schuuring, E. The involvement of the chromosome 11q13 region in human malignancies: cyclin D1 and EMS1 are two new candidate oncogenes--a review. *Gene* **159**, 83-96 (1995).

82. Zaharieva, B.M. et al. High-throughput tissue microarray analysis of 11q13 gene amplification (CCND1, FGF3, FGF4, EMS1) in urinary bladder cancer. *J Pathol* **201**, 603-8 (2003).

83. Huang, X., Gollin, S.M., Raja, S. & Godfrey, T.E. High-resolution mapping of the 11q13 amplicon and identification of a gene, TAOS1, that is amplified and overexpressed in oral cancer cells. *Proc Natl Acad Sci U S A* **99**, 11369-74 (2002).

84. Filmus, J. et al. Induction of cyclin D1 overexpression by activated ras. *Oncogene* **9**, 3627-33 (1994).

85. Sherr, C.J. & Roberts, J.M. CDK inhibitors: positive and negative regulators of G1-phase progression. *Genes Dev* **13**, 1501-12 (1999).

86. Sauter, E.R. et al. Cyclin D1 is a candidate oncogene in cutaneous melanoma. *Cancer Res* **62**, 3200-6 (2002).

87. Utikal, J., Udart, M., Leiter, U., Peter, R.U. & Krahn, G. Additional Cyclin D(1) gene copies associated with chromosome 11 aberrations in cutaneous malignant melanoma. *Int J Oncol* **26**, 597-605 (2005).

88. Patel, A.S., Schechter, G.L., Wasilenko, W.J. & Somers, K.D. Overexpression of EMS1/cortactin in NIH3T3 fibroblasts causes increased cell motility and invasion in vitro. *Oncogene* **16**, 3227-32 (1998).

89. Wu, H. & Parsons, J.T. Cortactin, an 80/85-kilodalton pp60src substrate, is a filamentous actin-binding protein enriched in the cell cortex. *J Cell Biol* **120**, 1417-26 (1993).

90. Pasello, G. et al. DNA copy number alterations correlate with survival of esophageal adenocarcinoma patients. *Mod Pathol* **22**, 58-65 (2009).

91. Timpson, P. et al. Aberrant expression of cortactin in head and neck squamous cell carcinoma cells is associated with enhanced cell proliferation and resistance to the epidermal growth factor receptor inhibitor gefitinib. *Cancer Res* **f67**, 9304-14 (2007).

92. Bringuier, P.P., Tamimi, Y., Schuuring, E. & Schalken, J. Expression of cyclin D1 and EMS1 in bladder tumours; relationship with chromosome 11q13 amplification. *Oncogene* **12**, 1747-53 (1996).

93. Harvell, J.D. et al. High-resolution array-based comparative genomic hybridization for distinguishing paraffin-embedded Spitz nevi and melanomas. *Diagn Mol Pathol* **13**, 22-5 (2004).

94. Gao, K., Lockwood, W.W., Li, J., Lam, W. & Li, G. Genomic analyses identify gene candidates for acquired irinotecan resistance in melanoma cells. *Int J Oncol* **32**, 1343-9 (2008).

95. Jonsson, G. et al. Genomic profiling of malignant melanoma using tiling-resolution arrayCGH. *Oncogene* **26**, 4738-48 (2007).

96. Moore, S.R. et al. Detection of copy number alterations in metastatic melanoma by a DNA fluorescence in situ hybridization probe panel and array comparative genomic hybridization: a southwest oncology group study (S9431). *Clin Cancer Res* **14**, 2927-35 (2008).

97. Sabatino, M. et al. Conservation of genetic alterations in recurrent melanoma supports the melanoma stem cell hypothesis. *Cancer Res* **68**, 122-31 (2008).

98. Albertson, D.G. et al. Quantitative mapping of amplicon structure by array CGH identifies CYP24 as a candidate oncogene. *Nat Genet* **25**, 144-6 (2000).

99. Hui, A.B., Lo, K.W., Teo, P.M., To, K.F. & Huang, D.P. Genome wide detection of oncogene amplifications in nasopharyngeal carcinoma by array based comparative genomic hybridization. *Int J Oncol* **20**, 467-73 (2002).

100. Pinkel, D. et al. High resolution analysis of DNA copy number variation using comparative genomic hybridization to microarrays. *Nat Genet* **20**, 207-11 (1998).

101. Takeo, S. et al. Examination of oncogene amplification by genomic DNA microarray in hepatocellular carcinomas: comparison with comparative genomic hybridization analysis. *Cancer Genet Cytogenet* **130**, 127-32 (2001).

102. Wilhelm, M. et al. Array-based comparative genomic hybridization for the differential diagnosis of renal cell cancer. *Cancer Res* **62**, 957-60 (2002).

103. O'Hagan, R.C. et al. Array comparative genome hybridization for tumor classification and gene discovery in mouse models of malignant melanoma. *Cancer Res* **63**, 5352-6 (2003).

104. Gast, A. et al. Somatic alterations in the melanoma genome: a high-resolution array-based comparative genomic hybridization study. *Genes Chromosomes Cancer* **49**, 733-45 (2010).

105. Li, W., Zhu, T. & Guan, K.L. Transformation potential of Ras isoforms correlates with activation of phosphatidylinositol 3-kinase but not ERK. *J Biol Chem* **279**, 37398-406 (2004).

106. Kabbarah, O. & Chin, L. Revealing the genomic heterogeneity of melanoma. *Cancer Cell* **8**, 439-41 (2005).

107. Pollock, P.M. et al. High frequency of BRAF mutations in nevi. *Nat Genet* **33**, 19-20 (2003).

108. Jiveskog, S., Ragnarsson-Olding, B., Platz, A. & Ringborg, U. N-ras mutations are common in melanomas from sun-exposed skin of humans but rare in mucosal membranes or unexposed skin. *J Invest Dermatol* **111**, 757-61 (1998).

109. van Elsas, A. et al. Relevance of ultraviolet-induced N-ras oncogene point mutations in development of primary human cutaneous melanoma. *Am J Pathol* **149**, 883-93 (1996).

110. Tanami, H. et al. Involvement of overexpressed wild-type BRAF in the growth of malignant melanoma cell lines. *Oncogene* **23**, 8796-804 (2004).

111. Platz, A., Egyhazi, S., Ringborg, U. & Hansson, J. Human cutaneous melanoma; a review of NRAS and BRAF mutation frequencies in relation to histogenetic subclass and body site. *Mol Oncol* **1**, 395-405 (2008).

112. Sebolt-Leopold, J.S. & Herrera, R. Targeting the mitogen-activated protein kinase cascade to treat cancer. *Nat Rev Cancer* **4**, 937-47 (2004).

113. Flaherty, K.T. et al. Inhibition of mutated, activated BRAF in metastatic melanoma. *N Engl J Med* **363**, 809-19 (2010).

114. Kim, J.K. & Diehl, J.A. Nuclear cyclin D1: an oncogenic driver in human cancer. *J Cell Physiol* **220**, 292-6 (2009).

115. Georgieva, J., Sinha, P. & Schadendorf, D. Expression of cyclins and cyclin dependent kinases in human benign and malignant melanocytic lesions. *J Clin Pathol* **54**, 229-35 (2001).

116. Lazar, V. et al. Characterization of candidate gene copy number alterations in the 11q13 region along with BRAF and NRAS mutations in human melanoma. *Mod Pathol* **22**, 1367-78 (2009).

117. Yang, S.X., Hewitt, S.M., Steinberg, S.M., Liewehr, D.J. & Swain, S.M. Expression levels of eIF4E, VEGF, and cyclin D1, and correlation of eIF4E with VEGF and cyclin D1 in multi-tumor tissue microarray. *Oncol Rep* **17**, 281-7 (2007).

118. Lazar, V. et al. Marked genetic differences between BRAF and NRAS mutated primary melanomas as revealed by array comparative genomic hybridization. *Melanoma Res* **22**, 202-14 (2012).

119. Musgrove, E.A., Caldon, C.E., Barraclough, J., Stone, A. & Sutherland, R.L. Cyclin D as a therapeutic target in cancer. *Nat Rev Cancer* **11**, 558-72 (2011).

120. Engelman, J.A., Luo, J. & Cantley, L.C. The evolution of phosphatidylinositol 3-kinases as regulators of growth and metabolism. *Nat Rev Genet* **7**, 606-19 (2006).

121. Xiao, D. & Singh, S.V. Diallyl trisulfide, a constituent of processed garlic, inactivates Akt to trigger mitochondrial translocation of BAD and caspase-mediated apoptosis in human prostate cancer cells. *Carcinogenesis* **27**, 533-40 (2006).

122. Yoon, K., Jung, E.J. & Lee, S.Y. TRAF6-mediated regulation of the PI3 kinase (PI3K)-Akt-GSK3beta cascade is required for TNF-induced cell survival. *Biochem Biophys Res Commun* **371**, 118-21 (2008).

123. Courtney, K.D., Corcoran, R.B. & Engelman, J.A. The PI3K pathway as drug target in human cancer. *J Clin Oncol* **28**, 1075-83 (2010).

124. Isshiki, K., Elder, D.E., Guerry, D. & Linnenbach, A.J. Chromosome 10 allelic loss in malignant melanoma. *Genes Chromosomes Cancer* **8**, 178-84 (1993).

125. Wu, H., Goel, V. & Haluska, F.G. PTEN signaling pathways in melanoma. *Oncogene* **22**, 3113-22 (2003).

126. Aguissa-Toure, A.H. & Li, G. Genetic alterations of PTEN in human melanoma. *Cell Mol Life Sci* (2011).

127. Tsao, H., Goel, V., Wu, H., Yang, G. & Haluska, F.G. Genetic interaction between NRAS and BRAF mutations and PTEN/MMAC1 inactivation in melanoma. *J Invest Dermatol* **122**, 337-41 (2004).

128. Liu, S., Ren, S., Howell, P., Fodstad, O. & Riker, A.I. Identification of novel epigenetically modified genes in human melanoma via promoter methylation gene profiling. *Pigment Cell Melanoma Res* **21**, 545-58 (2008).

129. Mertens, F., Johansson, B., Hoglund, M. & Mitelman, F. Chromosomal imbalance maps of malignant solid tumors: a cytogenetic survey of 3185 neoplasms. *Cancer Res* **57**, 2765-80 (1997).

130. Stahl, J.M. et al. Deregulated Akt3 activity promotes development of malignant melanoma. *Cancer Res* **64**, 7002-10 (2004).

131. Davies, M.A. et al. A novel AKT3 mutation in melanoma tumours and cell lines. *Br J Cancer* **99**, 1265-8 (2008).

132. Stark, M. & Hayward, N. Genome-wide loss of heterozygosity and copy number analysis in melanoma using high-density single-nucleotide polymorphism arrays. *Cancer Res* **67**, 2632-42 (2007).

133. Marone, R. et al. Targeting melanoma with dual phosphoinositide 3-kinase/mammalian target of rapamycin inhibitors. *Mol Cancer Res* **7**, 601-13 (2009).

134. Madhunapantula, S.V. & Robertson, G.P. Therapeutic Implications of Targeting AKT Signaling in Melanoma. *Enzyme Res* **2011**, 327923 (2011).

135. Sinnberg, T. et al. Inhibition of PI3K-AKT-mTOR signaling sensitizes melanoma cells to cisplatin and temozolomide. *J Invest Dermatol* **129**, 1500-15 (2009).

136. Robertson, G.P. Functional and therapeutic significance of Akt deregulation in malignant melanoma. *Cancer Metastasis Rev* **24**, 273-85 (2005).

137. Sharma, A.K. et al. Synthesis and anticancer activity comparison of phenylalkyl isoselenocyanates with corresponding naturally occurring and synthetic isothiocyanates. *J Med Chem* **51**, 7820-6 (2008).

138. Gaitonde, S. et al. BI-69A11-mediated inhibition of AKT leads to effective regression of xenograft melanoma. *Pigment Cell Melanoma Res* **22**, 187-95 (2009).

139. Huelsken, J. & Behrens, J. The Wnt signalling pathway. *J Cell Sci* **115**, 3977-8 (2002).

140. Komiya, Y. & Habas, R. Wnt signal transduction pathways. *Organogenesis* **4**, 68-75 (2008).

141. Larue, L. & Delmas, V. The WNT/Beta-catenin pathway in melanoma. *Front Biosci* **11**, 733-42 (2006).

142. Pham, K., Milovanovic, T., Barr, R.J., Truong, T. & Holcombe, R.F. Wnt ligand expression in malignant melanoma: pilot study indicating correlation with histopathological features. *Mol Pathol* **56**, 280-5 (2003).

143. You, L. et al. An anti-Wnt-2 monoclonal antibody induces apoptosis in malignant melanoma cells and inhibits tumor growth. *Cancer Res* **64**, 5385-9 (2004).

144. Lin, Y.C. et al. Wnt inhibitory factor-1 gene transfer inhibits melanoma cell growth. *Hum Gene Ther* **18**, 379-86 (2007).

145. Artavanis-Tsakonas, S., Rand, M.D. & Lake, R.J. Notch signaling: cell fate control and signal integration in development. *Science* **284**, 770-6 (1999).

146. Hoek, K. et al. Expression profiling reveals novel pathways in the transformation of melanocytes to melanomas. *Cancer Res* **64**, 5270-82 (2004).

147. Liu, Z.J. et al. Notch1 signaling promotes primary melanoma progression by activating mitogen-activated protein kinase/phosphatidylinositol 3-kinase-Akt pathways and up-regulating N-cadherin expression. *Cancer Res* **66**, 4182-90 (2006).

148. Massi, D. et al. Evidence for differential expression of Notch receptors and their ligands in melanocytic nevi and cutaneous malignant melanoma. *Mod Pathol* **19**, 246-54 (2006).

149. Huynh, C. et al. The novel gamma secretase inhibitor RO4929097 reduces the tumor initiating potential of melanoma. *PLoS One* **6**, e25264 (2011).

150. Lin, T.L. & Matsui, W. Hedgehog pathway as a drug target: Smoothened inhibitors in development. *Onco Targets Ther* **5**, 47-58 (2012).

151. Katoh, Y. & Katoh, M. Hedgehog target genes: mechanisms of carcinogenesis induced by aberrant hedgehog signaling activation. *Curr Mol Med* **9**, 873-86 (2009).

152. Alexaki, V.I. et al. GLI2-mediated melanoma invasion and metastasis. *J Natl Cancer Inst* **102**, 1148-59 (2010).

153. Das, S. et al. The hedgehog pathway transcription factor GLI1 promotes malignant behavior of cancer cells by up-regulating osteopontin. *J Biol Chem* **284**, 22888-97 (2009).

154. Li, C., Chi, S. & Xie, J. Hedgehog signaling in skin cancers. *Cell Signal* **23**, 1235-43 (2011).

155. Treszl, A. et al. Molecular cytogenetic characterization of a novel cell line established from a superficial spreading melanoma. *Front Biosci* **11**, 1844-53 (2006).

156. Jain, A.N. et al. Fully automatic quantification of microarray image data. *Genome Res* **12**, 325-32 (2002).

157. Lingjaerde, O.C., Baumbusch, L.O., Liestol, K., Glad, I.K. & Borresen-Dale, A.L. CGH-Explorer: a program for analysis of array-CGH data. *Bioinformatics* **21**, 821-2 (2005).

158. Lai, W.R., Johnson, M.D., Kucherlapati, R. & Park, P.J. Comparative analysis of algorithms for identifying amplifications and deletions in array CGH data. *Bioinformatics* **21**, 3763-70 (2005).

159. Tusher, V.G., Tibshirani, R. & Chu, G. Significance analysis of microarrays applied to the ionizing radiation response. *Proc Natl Acad Sci U S A* **98**, 5116-21 (2001).

160. Peter H. Westfall, S.S.Y. Resampling-based multiple testing: examples and methods for P value adjustment (John Wiley and Sons, New York, 1993).

161. Loo, L.W. et al. Array comparative genomic hybridization analysis of genomic alterations in breast cancer subtypes. *Cancer Res* **64**, 8541-9 (2004).

162. Stelling, J., Sauer, U., Szallasi, Z., Doyle, F.J., 3rd & Doyle, J. Robustness of cellular functions. *Cell* **118**, 675-85 (2004).

163. Korcsmaros, T. et al. Uniformly curated signaling pathways reveal tissue-specific cross-talks and support drug target discovery. *Bioinformatics* **26**, 2042-50 (2010).

164. Liaw A, W.M. Classification and regression by randomForest. *R News* **2**, 18-22 (2002).

165. Breiman, L. Random Forests. *Machine Learning* **45**, 5-32 (2001).

166. de Hoon, M.J., Imoto, S., Nolan, J. & Miyano, S. Open source clustering software. *Bioinformatics* **20**, 1453-4 (2004).

167. Saldanha, A. Java Treeview--extensible visualization of microarray data. *Bioinformatics* **20**, 3246-3248 (2004).

168. Zuker, M. Mfold web server for nucleic acid folding and hybridization prediction. *Nucleic Acids Res* **31**, 3406-15 (2003).

169. Pattyn, F., Speleman, F., De Paepe, A. & Vandesompele, J. RTPrimerDB: the real-time PCR primer and probe database. *Nucleic Acids Res* **31**, 122-3 (2003).

170. De Preter, K. et al. Quantification of MYCN, DDX1, and NAG gene copy number in neuroblastoma using a real-time quantitative PCR assay. *Mod Pathol* **15**, 159-66 (2002).

171. Pfaffl, M.W. et al. Real-time RT-PCR quantification of insulin-like growth factor (IGF)-1, IGF-1 receptor, IGF-2, IGF-2 receptor, insulin receptor, growth hormone receptor, IGF-binding proteins 1, 2 and 3 in the bovine species. *Domest Anim Endocrinol* **22**, 91-102 (2002).

172. Hoebeeck, J., Speleman, F. & Vandesompele, J. Real-time quantitative PCR as an alternative to Southern blot or fluorescence in situ hybridization for detection of gene copy number changes. *Methods Mol Biol* **353**, 205-26 (2007).

173. Hoebeeck, J. et al. Rapid detection of VHL exon deletions using real-time quantitative PCR. *Lab Invest* **85**, 24-33 (2005).

174. Bustin, S.A. et al. The MIQE guidelines: minimum information for publication of quantitative real-time PCR experiments. *Clin Chem* **55**, 611-22 (2009).

175. Pfaffl, M.W. A new mathematical model for relative quantification in real-time RT-PCR. *Nucleic Acids Res* **29**, e45 (2001).

176. Mak, W.B. & Fix, D. DNA sequence context affects UV-induced mutagenesis in Escherichia coli. *Mutat Res* **638**, 154-61 (2008).

177. Raman, V. et al. Compromised HOXA5 function can limit p53 expression in human breast tumours. *Nature* **405**, 974-8 (2000).

178. Hay, R., MacRae, E., Barber, D., Khalil, M. & Demetrick, D.J. BRAF mutations in melanocytic lesions and papillary thyroid carcinoma samples identified using melting curve analysis of polymerase chain reaction products. *Arch Pathol Lab Med* **131**, 1361-7 (2007).

179. Poynter, J.N. et al. BRAF and NRAS mutations in melanoma and melanocytic nevi. *Melanoma Res* **16**, 267-73 (2006).

180. Thomas, N.E. et al. Number of nevi and early-life ambient UV exposure are associated with BRAF-mutant melanoma. *Cancer Epidemiol Biomarkers Prev* **16**, 991-7 (2007).

181. Omholt, K., Platz, A., Kanter, L., Ringborg, U. & Hansson, J. NRAS and BRAF mutations arise early during melanoma pathogenesis and are preserved throughout tumor progression. *Clin Cancer Res* **9**, 6483-8 (2003).

182. Tavazoie, S.F. et al. Endogenous human microRNAs that suppress breast cancer metastasis. *Nature* **451**, 147-52 (2008).

183. Sellar, G.C. et al. OPCML at 11q25 is epigenetically inactivated and has tumor-suppressor function in epithelial ovarian cancer. *Nat Genet* **34**, 337-43 (2003).

184. Tsuchiya, E. et al. Three new regions on chromosome 17p13.3 distal to p53 with possible tumor suppressor gene involvement in lung cancer. *Jpn J Cancer Res* **91**, 589-96 (2000).

185. Chattopadhyay, P. et al. Loss of heterozygosity of a locus on 17p13.3, independent of p53, is associated with higher grades of astrocytic tumours. *Oncogene* **15**, 871-4 (1997).

186. Parrella, P. et al. HIC1 promoter methylation and 17p13.3 allelic loss in invasive ductal carcinoma of the breast. *Cancer Lett* **222**, 75-81 (2005).

187. Phillips, N.J. et al. Allelic deletion on chromosome 17p13.3 in early ovarian cancer. *Cancer Res* **56**, 606-11 (1996).

188. Schultz, D.C. et al. Identification of two candidate tumor suppressor genes on chromosome 17p13.3. *Cancer Res* **56**, 1997-2002 (1996).

189. Bruening, W. et al. Expression of OVCA1, a candidate tumor suppressor, is reduced in tumors and inhibits growth of ovarian cancer cells. *Cancer Res* **59**, 4973-83 (1999).

190. Huang, L. et al. MicroRNA-125b suppresses the development of bladder cancer by targeting E2F3. *Int J Cancer* **128**, 1758-69 (2011).

191. Diaz-Uriarte, R. & Alvarez de Andres, S. Gene selection and classification of microarray data using random forest. *BMC Bioinformatics* **7**, 3 (2006).

192. Gunther, E.C., Stone, D.J., Gerwien, R.W., Bento, P. & Heyes, M.P. Prediction of clinical drug efficacy by classification of drug-induced genomic expression profiles in vitro. *Proc Natl Acad Sci U S A* **100**, 9608-13 (2003).

193. Alvarez, S. et al. A predictor based on the somatic genomic changes of the BRCA1/BRCA2 breast cancer tumors identifies the non-BRCA1/BRCA2 tumors with BRCA1 promoter hypermethylation. *Clin Cancer Res* **11**, 1146-53 (2005).

194. Mandl, M., Slack, D.N. & Keyse, S.M. Specific inactivation and nuclear anchoring of extracellular signal-regulated kinase 2 by the inducible dual-specificity protein phosphatase DUSP5. *Mol Cell Biol* **25**, 1830-45 (2005).

195. Bessard, A. et al. RNAi-mediated ERK2 knockdown inhibits growth of tumor cells in vitro and in vivo. *Oncogene* **27**, 5315-25 (2008).

196. Ahmed, S.U. & Milner, J. Basal cancer cell survival involves JNK2 suppression of a novel JNK1/c-Jun/Bcl-3 apoptotic network. *PLoS One* **4**, e7305 (2009).

197. Tong, C. et al. c-Jun NH2-terminal kinase 1 plays a critical role in intestinal homeostasis and tumor suppression. *Am J Pathol* **171**, 297-303 (2007).

198. Rakosy, Z. et al. EGFR gene copy number alterations in primary cutaneous malignant melanomas are associated with poor prognosis. *Int J Cancer* **121**, 1729-37 (2007).

199. Hu, L., Zaloudek, C., Mills, G.B., Gray, J. & Jaffe, R.B. In vivo and in vitro ovarian carcinoma growth inhibition by a phosphatidylinositol 3-kinase inhibitor (LY294002). *Clin Cancer Res* **6**, 880-6 (2000).

200. Wiltshire, R.N., Dennis, T.R., Sondak, V.K., Meltzer, P.S. & Trent, J.M. Application of molecular cytogenetic techniques in a case study of human cutaneous metastatic melanoma. *Cancer Genet Cytogenet* **131**, 97-103 (2001).

201. Turner, N. & Grose, R. Fibroblast growth factor signalling: from development to cancer. *Nat Rev Cancer* **10**, 116-29 (2010).

202. Bastian, B.C. Understanding the progression of melanocytic neoplasia using genomic analysis: from fields to cancer. *Oncogene* **22**, 3081-6 (2003).

203. Smalley, K.S. et al. Increased cyclin D1 expression can mediate BRAF inhibitor resistance in BRAF V600E-mutated melanomas. *Mol Cancer Ther* **7**, 2876-83 (2008).

Keywords

primary melanoma, array comparative genomic hybridization, BRAF mutation, NRAS mutation, 11q13 chromosome region, CCND1 amplification, signaling pathways

Tárgyszavak

primer melanoma, komparatív genomiális hibridizáció, BRAF mutáció, NRAS mutáció, 11q13 kromoszómális régió. CCND1 amplifikáció, jelátviteli útvonalak

Acknowledgments

This work was carried out at the Department of Preventive Medicine, Faculty of Public Health, Medical and Health Science Center, University of Debrecen, Hungary, during 2005-2009. These researches was supported by the Hungarian National Research Fund (OTKA K75191), the National Research and Development Program, Hungary (NKFP1-00003/2005), the Hungarian Academy of Sciences (grant number 2006TKI247), the Hungarian Medical Research Council (193/99-ETT) and the TÁMOP 4.2.1./B-09/1/KONV-2010-0007 project, the project is implemented through the New Hungary Development Plan, co-financed by the European Social Fund and the European Regional Development Fund.

I am deeply grateful to Professor Margit Balázs for steering me towards the field of melanoma research, and for guiding me as a supervisor with vast knowledge and tolerant patience. Moreover I wish to express my gratitude to Professor Róza Ádány, the Head of the Department of Preventive Medicine, for giving me the excellent opportunity for scientific work during these years.

I also express my deep gratitude to my co-authors for rewarding collaboration:

- Ágnes Bégány, M.D., Ph.D., and Gabriella Emri, M.D., Ph.D., from the Department of Dermatology, Faculty of Medicine, Medical and Health Science Center University of Debrecen, Debrecen, Hungary for providing and reassessing the primary melanoma samples.
- Réka Tóth, Ph.D. from the Department of Preventive Medicine, Faculty of Public Health, for sharing many evenings with me at the PCR laboratory and for stimulating conversations.
- Balázs Szappanos and Gábor Boross M.Sc., from the Evolutionary Systems Biology Group, Institute of Biochemistry, Biological Research Centre, Szeged, Hungary, for always being ready to help when the statistics were particularly challenging.

I would also like to give my thanks to the rest of this great research group: Laura Vízkeleti, Szilvia Ecsedi for their advice and friendship during my time there. I wish to thank all my colleagues and staff at the Department of Preventive Medicine for their friendship and for creating a stimulating work atmosphere.